Further Studies on the Highly Active Des-C-Ring and Aromatic-D-Ring Analogues of 1,25-Dihydroxyvitamin D3 (Calcitriol): Refinement of the Side Chain

Araceli Zárate-Ruíz, Samuel Seoane, Carole Peluso-Iltis, Stefan Peters, Carlos Gregorio, Thierry Guiberteau, Miguel A Maestro, Román Pérez-Fernández, Natacha Rochel, Antonio Mouriño

Further Studies on the Highly Active Des-C-Ring and Aromatic-D-Ring Analogs of 1α,25-Dihydroxyvitamin D_3 (Calcitriol): Refinement of the Side Chain.

Araceli Zárate-Ruíz,[§,¶] Samuel Seoane,[‡,¶] Carole Peluso-Iltis,[#] Stefan Peters,[§] Carlos Gregorio,[§] Thierry Guiberteau,[¤] Miguel Maestro,[γ] Román Pérez-Fernández,[‡,] Natacha Rochel,[#,*] Antonio Mouriño[§,*]*

§Department of Organic Chemistry, Research Laboratory Ignacio Ribas, University of Santiago de Compostela, Avda. de las Ciencias s/n, 15782 Santiago de Compostela, Spain

‡Department of Physiology–Center for Research in Molecular Medicine and Chronic Diseases (CIMUS), University of Santiago de Compostela, Avda. Barcelona s/n, 15706 Santiago de Compostela, Spain

#Institut de Génétique et de Biologie Moléculaire et Cellulaire (IGBMC), 67400 Illkirch, France; Institut National de La Santé et de La Recherche Médicale (INSERM), U1258, 67400 Illkirch, France; Centre National de Recherche Scientifique (CNRS), UMR7104, 67400 Illkirch, France; Université de Strasbourg, 67400 Illkirch, France

¤Laboratoire ICube - Université de Strasbourg, CNRS UMR 7357, 67000 Strasbourg, France

γ Department of Chemistry-CICA, University of A Coruña, Campus da Zapateira s/n, 15071 A Coruña, Spain

¶ Araceli Zárate-Ruíz and Samuel Seoane contributed equally to this work.

Corresponding authors:

* E-mail: roman.perez.fernandez@usc.es

* E-mail: rochel@igbmc.fr

* E-mail: antonio.mourino@usc.es

Table of Contents Graphic

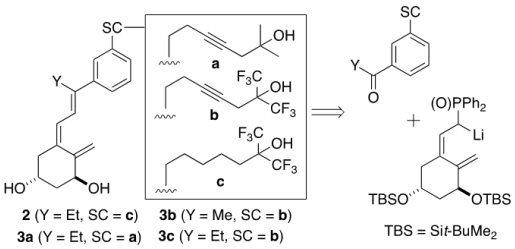

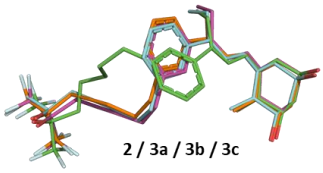

-Strong activation of *CYP24A1* gene
-Normocalcemic activities
-Decrease cell proliferation
-Decrease cell proliferation when combined with cisplatin
-Stabilize VDR interactions

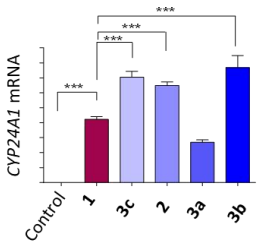

ABSTRACT

Current efforts in the vitamin D field are directed towards the development of highly anti-proliferative yet non-calcemic analogs of the natural hormone 1α,25-dihydroxyvitamin D_3 (1,25D_3). We have recently reported the design, synthesis, biological evaluation, and crystal structures of a series of novel analogs that both lack the steroidal C-ring and have a *m*-phenylene ring replacing the steroidal cyclopentane D-ring. We have now investigated the potentiating effects of incorporating selected modifications (hexafluorination and/or an internal triple bond) within the steroidal side chain in our series. An alternative synthetic strategy (Wittig-Horner approach instead of our previously used Pd-catalyzed tandem cyclization/cross coupling) for the construction of the vitamin D triene system was found convenient for the target compounds **2**, **3a**, **3b** and **3c** of this report. These modifications enhance VDR interactions and consequently VDR associated biological properties compared to parental PG-136 compound, while maintaining normal calcium levels.

KEYWORDS: noncalcemic des-C-ring vitamin D analogs; aromatic D-ring analogs; calcemia; antiproliferation; design; synthesis; crystal structure.

INTRODUCTION

The bioactive vitamin D_3, 1α,25-dihydroxyvitamin D_3 (**1**, calcitriol, $1,25D_3$) is a secosteroid hormone controlling calcium absorption and reabsorption in intestine and kidney, respectively, and promotes calcium mobilization from bones.[1-2] The activities of $1,25D_3$ are mediated by the vitamin D nuclear receptor (VDR), which belongs to the superfamily of nuclear receptors. VDR heterodimerizes with retinoid X receptors (RXRs) and binds DNA sites located in regulated target genes. Vitamin D signaling is involved in various physiological and pathophysiological mechanisms.[3] In addition to the role in the regulation of mineral homeostasis, $1,25D_3$ regulates growth and differentiation of many cell types, and displays immuno-regulatory and anti-inflammatory activities.[4] $1,25D_3$ deficiency and loss-of-function VDR variants induce rickets.[5] Moreover, low $1,25D_3$ circulating levels and/or low VDR expression correlate with the onset and severity of several auto-immune diseases and various cancers.[6] The antiproliferative effect of $1,25D_3$ has been demonstrated in cell culture and in animal models of various cancers.[7-8]

Despite wide potential clinical applications, $1,25D_3$ benefit in the clinics is limited, mainly because the required doses induce hypercalcemia.[9] In order to potentiate beneficial properties of $1,25D_3$, and/or reduce their hypercalcemic side effects, thousands of analogs were synthesized, and few of them went to the clinics.[10-11] Most of the $1,25D_3$ analogs developed to date are modified in the side chain[12] and A-ring,[13] but only a few having structural alterations in the C-ring and/or D-ring have been developed due to synthetic difficulties.[14-18] Biological studies on $1,25D_3$ analogs that lack the D-ring,[19] C-ring,[19] the bicyclic CD-ring,[20] or are modified on the C- or D-rings,[21-23] show that the natural CD-core of $1,25D_3$ is not necessary for biological activity and its modification can reduce the calcemic activity.

We have recently developed three $1,25D_3$ analogs that lack the C-ring and possess an aromatic D-ring.[24,25] **PG-136** (Figure 1) is an example of this new class highly active and non-calcemic $1,25D_3$-analogs.[24] Here we describe the *in-silico* design, synthesis, biological evaluation and structural characterization of the new $1,25D_3$ analogs **2, 3a, 3b, and 3c**, which lack the natural steroidal C-ring and possess an aromatic *m*-phenylene-

ring replacing the natural five-membered D-ring. These new compounds incorporate modifications known to increase the VDR interactions, either a rigidified alkyne side chain or fluorine atoms at the terminus of the side chain. The presence of a triple bond in the side chain of 1,25D_3 analogs has been associated with enzymatic block of hydroxylation at C-23 and C-24, but not at C-26.[26-28] Side chain fluorination has been used to synthesize 1,25D_3 analogs metabolically stable and improved anti-cancer activity. [29,30]

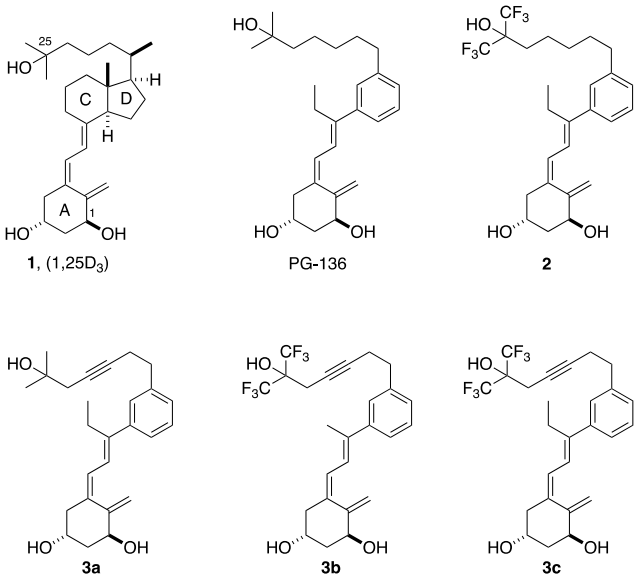

Figure 1. Structures of 1α,25-dihydroxyvitamin D_3 (**1**, 1,25D_3, calcitriol), analog **PG-136,** and target des-C-ring and aromatic-D-ring analog **2**, having fluorine atoms at the terminus of the side chain, and **3a**, **3b**, and **3c**, bearing an alkyne side chain with or without fluorine atoms at the terminus of the side chain.

RESULTS AND DISCUSSION

Docking Studies.

For first insights, docking studies using AutoDock VINA 1.2.0[31] were conducted with compounds **2** and **3a-c**. As target for the docking, we used the human hVDR ligand binding domain (LBD)-1,25D_3 crystal structure (PDB 1DB1)[32] that corresponds to a truncated construct, which lacks the flexible insertion domain in the LBD. For comparison, the scoring was normalized on 1,25D_3. The lowest scoring was reached by analog **3a** (82%) while **3b** and **3c** reached a score of 94% (Figure 2). Compound **2** showed

a score of 91% in comparison to 1,25D_3. All four analogs formed the crucial hydrogen bridges with His305 and His397. The other important hydrogen bonding interactions of the A-ring with Tyr143, Ser237, Arg274 and with Ser278 were also preserved for all compounds. The aromatic system of the compounds took the position of the D-ring of the natural hormone and the methyl or ethyl substituent at C-8 filled the position of the C-ring. This central moiety could potentially form a π-π-stacking with Trp286, however only the group attached at C-8 interact with Trp286 at a distance of 3.7 Å. The A-Ring of the docked analogs was also in the same position, but showed slight rotation resulting in a different positioning of the 1-OH group. Another difference in comparison to 1,25D_3 is the position of the aryl side chain. Especially the alkyne-containing side chains are oriented towards helix 6 (H6), while keeping the OH-group at the tip in position to form the important hydrogen bridge with the histidines. Since the docked poses for all four analogs are highly overlapping, the differences in the scoring seem to derive from the stronger hydrogen donor capability of the $(CF_3)_2$COH-group compared to the $(CH_3)_2$COH-group (Figure 2).

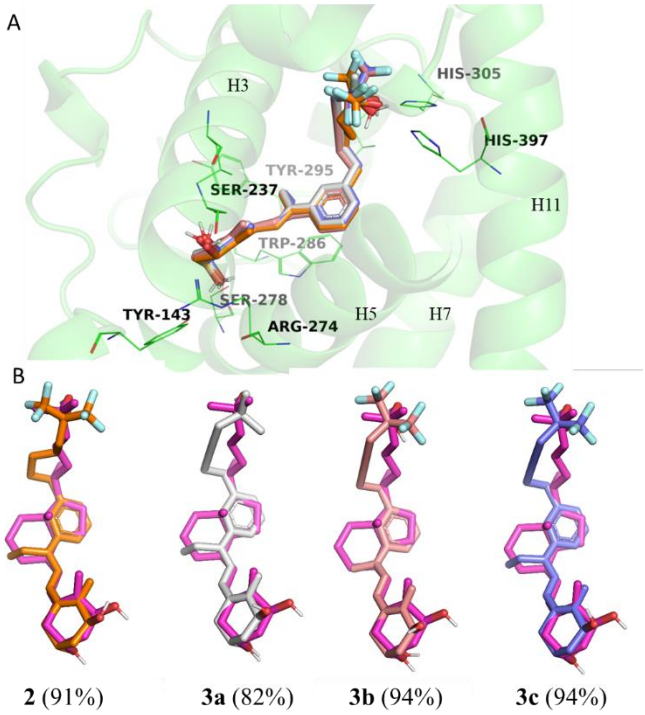

Figure 2. (**A**) Superposition of the docked poses of **2** (orange), **3a** (white), **3b** (beige) and **3c** (blue) in the binding pocket of human 1,25D_3-hVDR LBD (green, PDB 1DB1). Important AA residues and helices are marked. (**B**) Single overlays of **2** and **3a-c** with 1,25D_3 extracted from PDB 1DB1 (purple). The scoring relative to 1,25D_3 in brackets.

To further explore the potential binding of these analogs, molecular dynamic (MD) calculations were performed. In our study, we used the YASARA suite[33,34] with the Amber14 ForceField and a simulation time of 20 ns comparable to our previous study of des-C-ring-aryl-D-ring compounds.[25] The results for the different analogs varied significantly in this study. The pose of compound **2** showed only slight differences after the MD calculations with the aryl ring and the $(CF_3)_2COH$-group staying almost in the same position compared to the docking studies (Figure 3A). Also notable was the change of the orientation of the ethyl group at C-8. The shape of the receptor did not change significantly during this simulation. More changes were observed for the MD simulated pose of **3c** (rmsd = 0.973 Å) where the position of the A-ring and the triene system were comparable to the docked pose, however the aryl ring was twisted also affecting the position of the alkyne side chain (Figure 3D). During this simulation helix 7 shifted about 2 Å towards the compound resulting also in a change of the position of His305 by 1.4 Å. Helix 11 remained unchanged, however, the heterocycle of His397 shifted by 3 Å in the direction of helix 12. Even greater differences were observed after the simulation of **3a** with significant changes in the position of the aryl-ring, the ethyl group at C-8 and shifts of helix 5 (by 2 Å), helix 7 (by 1.6 Å) and helix 11 (by 1.7 Å) (Figure 3C). Additionally, His305 was shifted by 1.5 Å towards the compound and His397 was shifted by 2 Å away from the compound, resulting in significant differences of the binding pocket compared to the crystal structure PDB 1DB1 (rsmd = 1.162 Å). Simulation of **3b** induced lesser changes of the conformation of the receptor, but the orientation of the ligand changed dramatically (Figure 3B). The aromatic ring was in a perpendicular position compared to the docked pose and the C-8-methyl group was now oriented towards helix 3 instead of helix 6 resulting in a flip of the core structure. Additionally, the A-ring was twisted by 1.6 Å and the polar side chain head was shifted by 2.5 Å resulting in a rmsd of 1.122 Å compared to the docked pose.

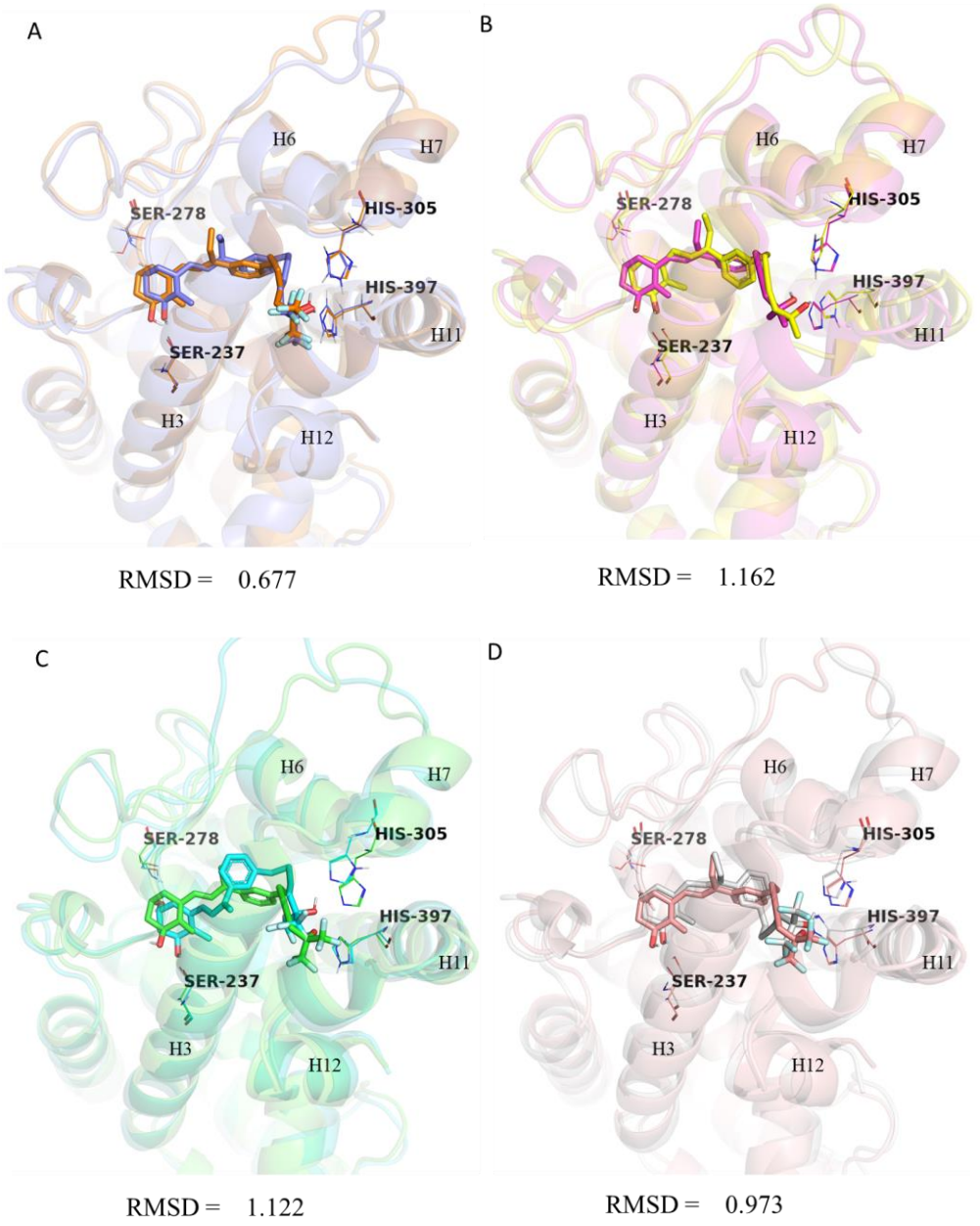

Figure 3. (**A**) Superposition of the docking pose of **2** (orange) in the 1DB1 X-ray structure (orange) with the MD-simulated structure of **2** in 1,25D$_3$-hVDR (blue). Residues forming hydrogen bonds with the hydroxyl groups of the ligands are highlighted. (**B**) Superposition of the docking pose of **3a** (yellow) in the 1DB1 X-ray structure (yellow) with the MD-simulated structure of **3a** in 1,25D$_3$-hVDR (purple). (**C**) Superposition of the docking pose of **3b** (green) in the 1DB1 X-ray structure (green) with the MD-simulated structure of **3b** in 1,25D$_3$-hVDR (turquoise). (**D**) Superposition of the docking pose of **3c** (beige) in the 1DB1 X-ray structure (beige) with the MD-simulated structure of **3c** in 1,25D$_3$-hVDR (white).

Retrosynthetic analysis.

For comparison with previous synthetic approaches to similar compounds,[24,25] we chose the Wittig-Horner coupling[35] between ketones **5a** and the phosphine oxide anion **4b** as the key step for the stereoselective formation of the respective vitamin D trienes of target compounds **2** and **3** (Scheme 1) with the expectation that the final target compounds could be separated by chromatography from the corresponding unnatural triene counterparts. Ketone **5a** was envisioned to arise from corresponding alkynes **6.** Ketones **8** would also arise from alkynes **6** through protected alcohols **9**. Alkynes **6** would be prepared from commercial bromoaldehyde **7**.

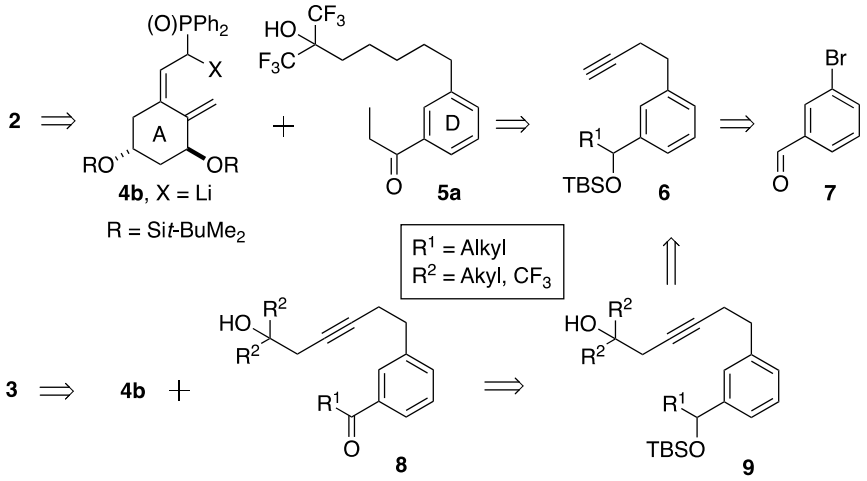

Scheme 1. Retrosynthetic analysis for target 1,25D$_3$-analogs **2** and **3**.

Synthesis of alkynyl intermediates 6 and 9. Heck reaction between bromoaldehyde **7** and ethyl acrylate in the presence of palladium acetate, triphenyl phosphine, and triethyl amine in DMF, provided the α,β-unsaturated ester **10** in 95% yield (Scheme 2). Addition of ethylmagnesium bromide or methylmagnesium bromide to **10** in Et_2O gave alcohols **11a** (85%) and **11b** (80%), respectively. Hydrogenation of **11a** and **11b** in the presence of catalytic Pd/C in CH_2Cl_2 afforded hydroxyesters **12a** (91%) and **12b (**90%), respectively. Individual protection of these alcohols with *tert*-butyldimethylsilyl chloride in the presence of imidazole in DMF gave the protected alcohols **13a** (98%) and **13b** (96%), respectively, whose reduction with diisobutylaluminum hydride in CH_2Cl_2 provided the corresponding aldehydes **14a** (87%) and **14b** (90%). Corey-Fuchs chain extension[36] on these aldehydes with zinc, carbon tetrabromide and triphenyl phosphine in dichloromethane afforded the corresponding dibromides **15a** (87%) and **15b** (89%), which were converted to alkynes **6a** (94%) and **6b** (94%) by treatment with *n*-buthyllithium in THF. Metalation of **6a** with *n*-hexyllithium in diethyl ether followed by

reaction of the resulting lithium derivative with epoxide **16a** (R^2 = Me) provided the tertiary alcohol **9a** in 97% yield. Same protocol was used for the preparation of alcohols **9b** (90%) and **9c** (91%) from the respective alkynes **6a** and **6b** using epoxide **16b** (R^2 = CF_3).

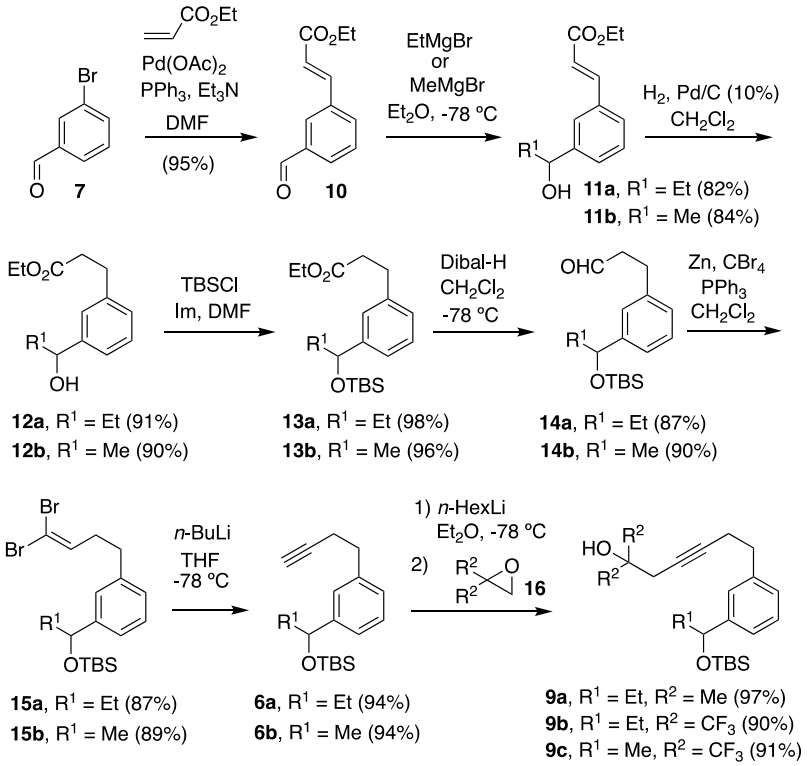

Scheme 2. Synthesis of intermediates **6** and **9** from aldehyde **7**.

Synthesis of vitamin D analog 2. Hydrogenation of alkyne **9b** in the presence of Adams catalyst in THF provided alcohol **17a** (98%), which was desilylated to alcohol **17b** (99%) with *n*-tetrabutylammoniun fluoride in THF (Scheme 3). Oxidation of **17b** with Dess-Martin periodinane[37] in dichloromethane gave ketone **5a** (92%), which was protected with triethylsilyl chloride in the presence of imidazole in dimethylformamide to afford the desired ketone **5b** (92%). Wittig-Horner coupling between ketone **5b** and and phosphine oxide anion **4b** in THF provided a mixture of protected analog **2** and its (7*Z*)-isomer in 68% yield (4:1 ratio as judged by the ^{1}H NMR of the corresponding crude mixture). Desilylation with *n*-tetrabutylammoniun fluoride in THF and HPLC separation from the (7*Z*)-isomer afforded the desired vitamin D analog **2** in 56% yield (two steps) (52% overall yield from **9b**, 6 steps).

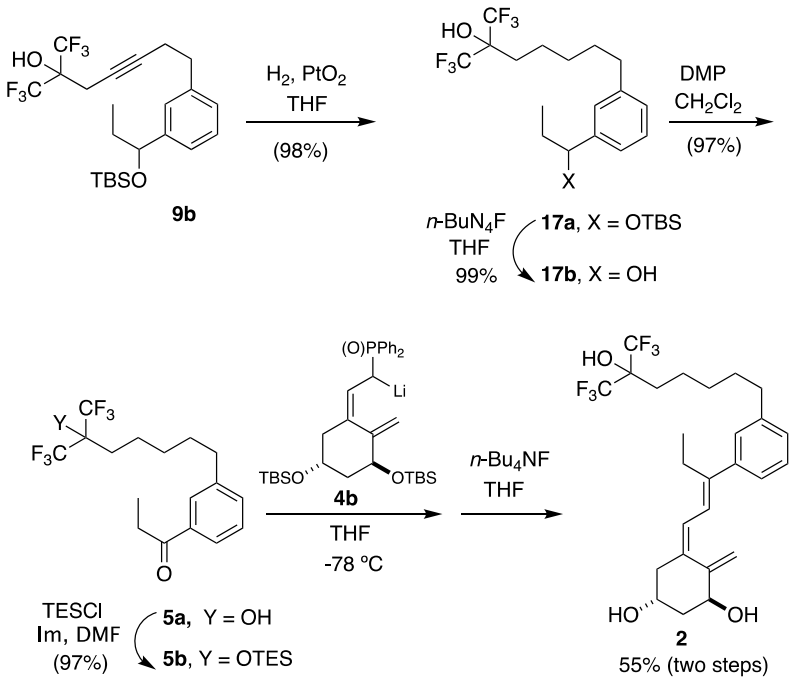

Scheme 3. Synthesis of vitamin D analog **2**.

Synthesis of target vitamin D analogs 3a, 3b, and 3c started with alkynes **9a-c**, which were deprotected with *n*-tetrabutylammonium fluoride in THF to the respective diols **18a** (97%), **18b** (94%), and **18c** (90%) (Scheme 4). These alcohols were individually oxidized with Dess-Martin periodinane in dichloromethane to provide the corresponding ketones **8a** (91%), **8b** (94%), and **8c** (95%). Reaction of the tertiary hydroxyl group of these ketones was accomplished with triethylsilyl chloride in the presence of imidazole in dimethylformamide-dichloromethane to furnish the protected ketones **19a** (99%), **19b** (90%), and **19c** (91%). Finally, these ketones were reacted with phosphine oxide anion **4b** as above to afford, after desilylation and HPLC separation from the corresponding (7*Z*)-isomers (20%), the corresponding target vitamin D analogs **3a** (31%), **3b** (27%), and **3c** (31%). The Wittig-Horner coupling of the unsaturated hexafluoro-ketones with the phosphine oxide anion occurred with partial deprotection of the –SiTES group and produced the natural vitamin D triene system and the (7*Z*)-isomer in a 4:1 ratio as judged by the ^{1}H NMR of the corresponding crude mixtures.

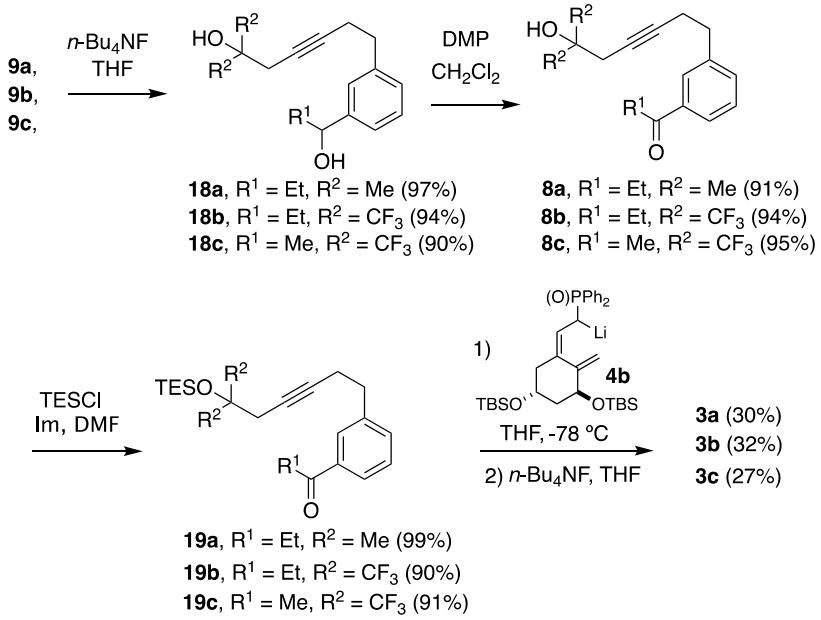

Scheme 4. Synthesis of vitamin D analogs **3a**, **3b**, and **3c.**

Biological Assays.

We analyzed the ability of the **2**, **3a**, **3b** and **3c** analogs to bind VDR by competitive binding assay (Figure 4A). VDR binding affinities of compounds **2, 3a** and **3c** are similar to that of 1,25D$_3$, whereas for **3b** it is approximately 10 times lower than 1,25D$_3$. Compound **2** that is the hexafluoro version of the previously described **PG-136**, binds 10 times more strongly to VDR than its parental compound.[24] Transcriptional activation of a vitamin D target gene *CYP24A1* (24-hydroxylase, a well-known 1,25D$_3$ target gene) by the analogs was evaluated by RT-PCR. The **2**, **3a**-**c** analogs and 1,25D$_3$ induced strong activation of the *CYP24A1*, as measured in mRNA expression after 48 h of treatment (Figure 4B). Of note, transcript levels induced by **2**, **3b** and **3c** were significantly higher than those induced by 1,25D$_3$ or the previously characterized des-C-ring and aromatic-D-ring analogs.[24] Calcium serum levels were evaluated in mice after i.p. injection of the **2**, **3a-c** analogs, and 1,25D$_3$ (Figure 4C). Our data indicated that analogs administration did not significantly raise calcium levels, in relation to vehicle-treated mice. In contrast, administration of 1,25D$_3$ significantly ($P<0.001$) increases calcium levels as compared with controls. Body weight is significantly ($P<0.05$) reduced after three weeks of treatment with 1,25D$_3$, as compared with the **2**, **3a-c** analogs (Figure 4D). These normocalcemic activities of the new analogs were already observed for the previously characterized des-C-ring and aromatic-D-ring analogs.

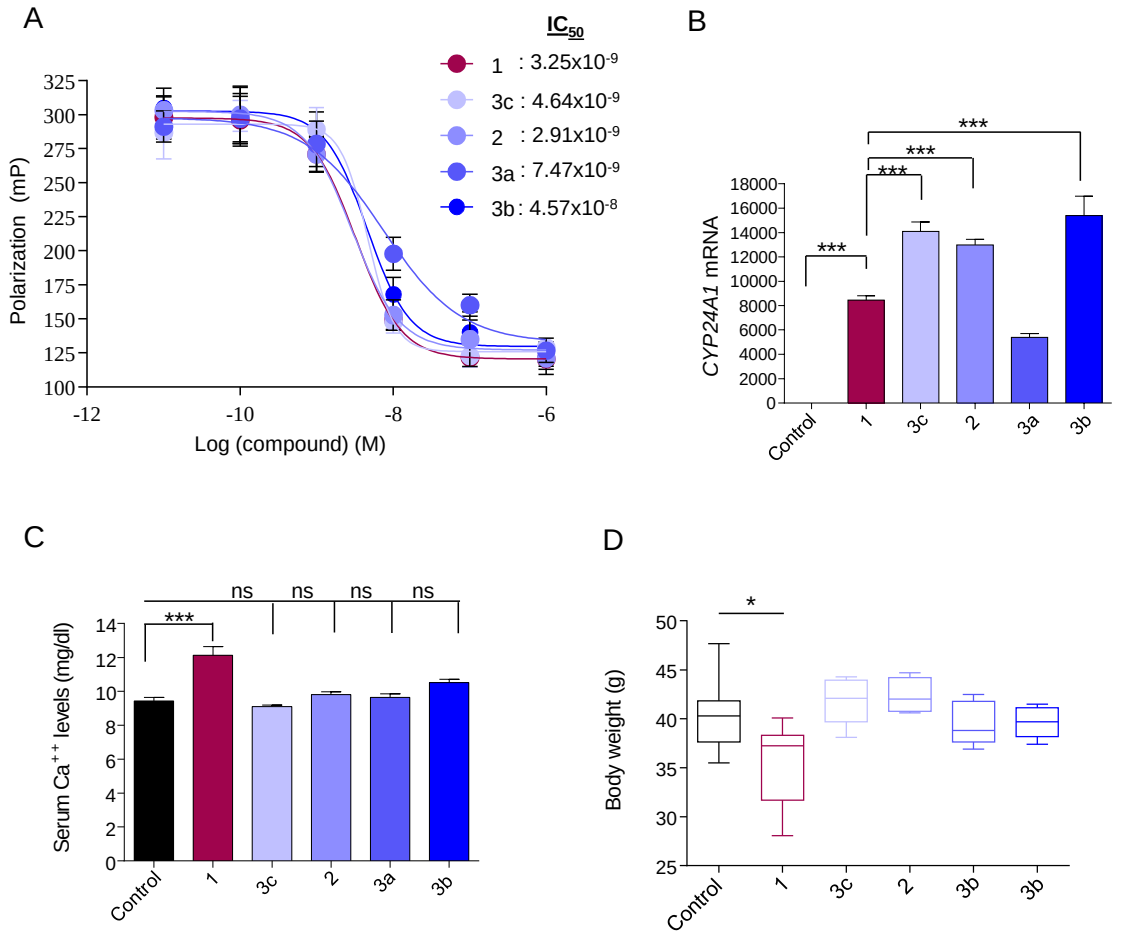

Figure 4. Biological properties of the vitamin D analogs. **(A)** Competitive binding of $1,25D_3$ **(1)** as control, and the **2**, **3a**, **3b**, and **3c** analogs to full-length human VDR. IC50 values are derived from dose–response curves (10^{-11} to 10^{-6} M). **(B)** Real-time PCR of the *CYP24A1* mRNA levels in MCF-7 cells treated for 48h with ethanol (control), $1,25D_3$, **2**, **3a**, **3b** and **3c** analogs at 10^{-7} M. **(C)** Calcemic activity. Mice were treated every other day for 21 days with sesame oil (control), and 0.3 μg/kg of 1,25D, **2**, **3a**, **3b** and **3c**. (X+SD, n=5 per group). **(D)** Box plot of the weight of mice treated as in C) on day 21. ns= not significant, * = P<0.05, *** = P<0.001.

We next evaluated the activity of the analogs to differentiate normal human keratinocyte HaCaT cells. All four compounds at 10^{-7} M have pro-differentiating effects similar to $1,25D_3$, as shown for example in the formation of compact epithelioid islands (Figure 5A). In addition, the four analogs induced the expression of Cadherin 1 (Figure 5B), an important intercellular adhesion protein in epithelial cells, similar to $1,25D_3$ at 10^{-7} M. Given the upregulation of Cadherin 1 expression and the differentiation activity of the analogs, we tested the antiproliferative effects of these compounds in the triple-negative

highly metastatic human breast adenocarcinoma MDA-MB-231 cell line. We found a significant ($P<0.001$) decrease in cell proliferation after treatment with $1,25D_3$ as compared to controls, being greater in cells treated with the **2**, **3a**, **3b** and **3c** analogs (Figure 5C). To further evaluate whether the vitamin D analogs could increase the effects of cisplatin, a well-known anti-tumoral drug in the subtype of triple-negative breast cancer (TNBC), the MDA-MB-231 cells were treated with the **2**, **3a-c** analogs at 10^{-7} M with and without cisplatin (25 μM). Our results indicated that both, $1,25D_3$ and the analogs potentiate the effect of cisplatin (Figure 5C). Finally, using three-dimensional cultures of MDA-MB-231 cells (Figure 5D) we show that the vitamin D analogs significantly ($P<0.001$) decrease cell proliferation when combined with cisplatin as compared to cisplatin alone.

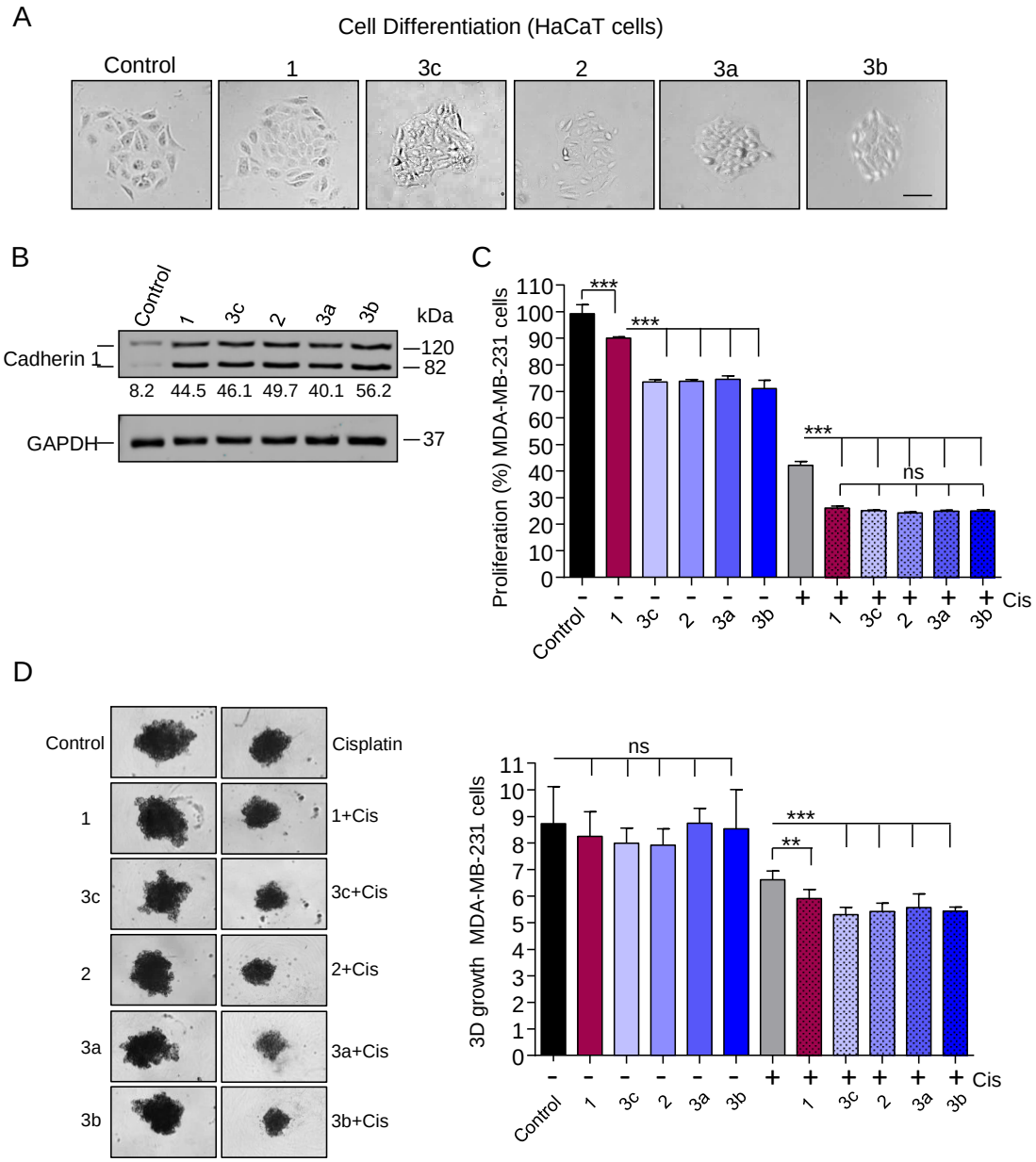

Figure 5. Biological functions of the vitamin D analogs. (**A**) Representative phase-contrast micrographs of differentiation of HaCaT cells treated with each compound at 10^{-7} M for 48 h. Controls were treated with ethanol. Scale bar=100μm. (**B**) Western blot of Cadherin 1 and GAPDH (used as control) in MCF-7 cells treated with each compound at 10^{-7} M for 48h. (**C**) MDA-MB-231 cells were cultured with ethanol (as control), **1**, **2**, **3a**, **3b**, and **3c** analogs (10^{-7} M) alone, and combined with cisplatin (25 μM). Two days later, cell proliferation was evaluated. The graph represents the percent inhibition of proliferation of each compound compared to normalized control (treated with ethanol, 100%). (**D**) Three-dimensional growth of MDA-MB-231 cells cultured for 4 days, and treated for 6 days with ethanol, **1**, **2**, **3a**, **3b** and **3c** analogs (10^{-7} M, every other day) without or with cisplatin (25 μM). Sphere growth of 3D cultures was quantified and represented as relative units (RU). Values are plotted as mean ± SD. ns= not significant, * = $P < 0.05$, ** = $P < 0.01$, *** = $P < 0.001$.

In summary, the biological evaluation of the **2**, **3a**, **3b,** and **3c** analogs shows that they share a similar mechanism of action to $1,25D_3$ in human breast cancer cells while having normocalcemic activities, which could indicate therapeutic activity in breast cancer.

Crystal Structures of VDR LBD Complexes.

The crystal structures of the LBD of zebrafish-VDR [(zVDR) LBD] in complex with the ligands **2**, **3a**, **3b** and **3c** and NCOA2 coactivator peptide, were solved and refined at a resolution of 2.3 Å, 2.0 Å, 2.3 Å, and 2.8 Å, respectively (see supplementary table 1 for details). Note, that the human- and zebrafish-VDR ligand binding pockets are lined with identical residues and have homologous structures.[38,39] In addition, both VDR species have similar dynamic properties upon ligand binding.[40,41] These crystal structures corroborated substantially the docking data. The VDR complexes exhibit the VDR canonical agonist conformation as the previously solved crystallographic structures VDR in complex with agonist ligands.[11] Some uncertainty in the positioning of part of the side chain remains for some analogs (Supplementary Figure 2). The alkyl chains attached to C8 of the triene system and the aromatic ring occupy the space filled by the CD-rings of the natural $1,25D_3$ ligand (Figure 6). The hydroxyl groups of the compounds form H-bonds with a pair of residues for each OH group, similarly to $1,25D_3$ and to the **PG-136** analog (Figure 6B-F).

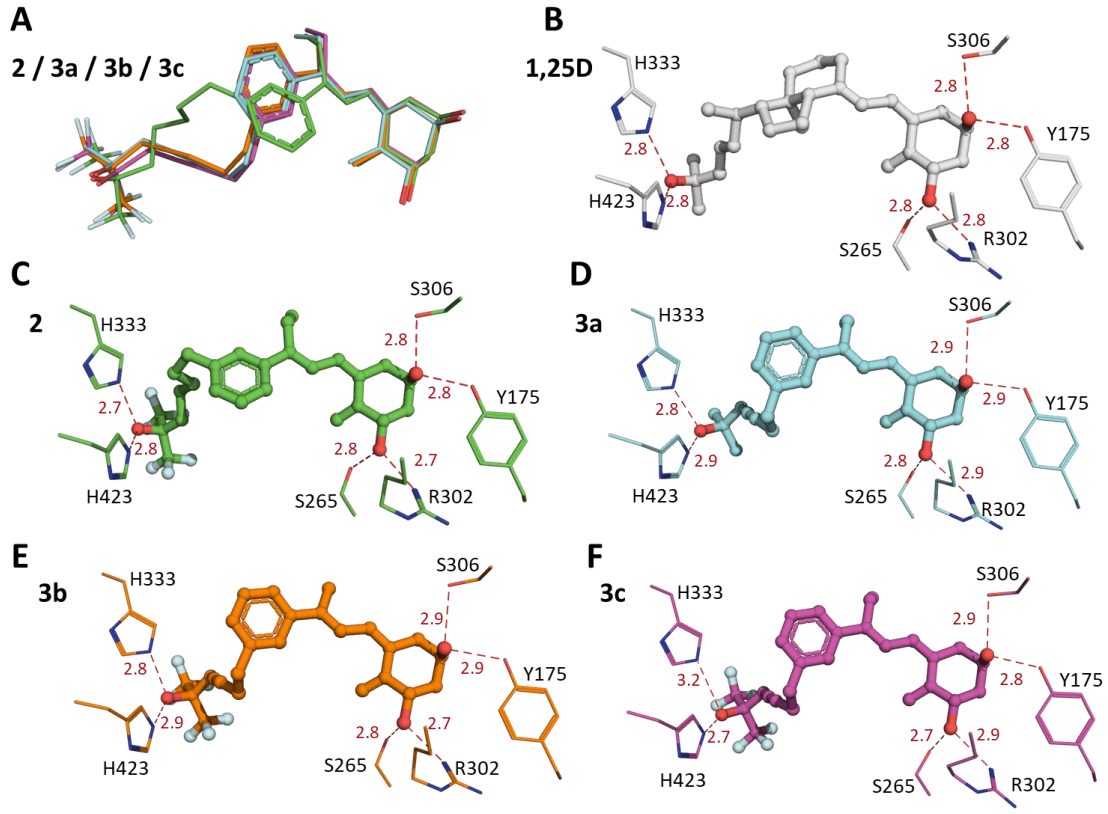

Figure 6. X-ray crystal structures of zVDR LBD in complex with analogs **2** (PDB 8PWF), **3a** (PDB 8PWE), **3b** (PDB 8PWM) and **3c** (PDB 8PWD). (**A**) Ligands **2** (green), **3a** (cyan), **3b** (orange) and **3c** (pink) superimposed. (**B**) Hydrogen bonds formed by $1,25D_3$ are shown by red dotted lines. (**C-F**) Hydrogen bonds formed by **2** (**C**), **3a** (**D**), **3b** (**E**) and **3c** (**F**). Indicated distances are in angstroms.

The compounds mimic the conformation of $1,25D_3$ and form the hydrophobic interactions of $1,25D_3$ (Figure 7A-D and supplementary table 2). In all VDR complexes, zTrp314 does not interact with the aromatic moiety of the analogs but contacts the C8-alkyl chains (supplementary table 2). Compound **2** form tighter interactions with zIle299 and zMet300 (Figure 7A), similarly to its parental compound **PG-136**.[24] The fluorine atoms at the terminus of the side chain allow analog **2** to interact more strongly with residues of helix 3, loop 6-7 and Cter, thus further stabilizing the active conformation and explaining the more potent activity of compound **2** compared to **PG-136.**[25] In order to maintain the hydrogen bonds formed by the 25-OH group, compounds **3** that incorporate a rigidified alkyne side chain, require a different conformation of the aromatic ring and their side chain are lining the opposite side of the pocket (Figure 6A). These differences lead to

stronger interactions of the compounds **3** with zVal262 and zIle296 (Figure 7B-D). Among the three compounds of the series **3,** the non-fluorinated compound **3a** form less interactions with C-terminal residues and stabilize the less efficiently the VDR active conformation (Figure 7B), whereas the fluorine atoms of the compounds **3b** and **3c** interact more strongly with residues of helix 3, loop 6-7 and C-terminal region, notably with zVal444 and zPhe448 in helix 12 (Figure 7C-D).

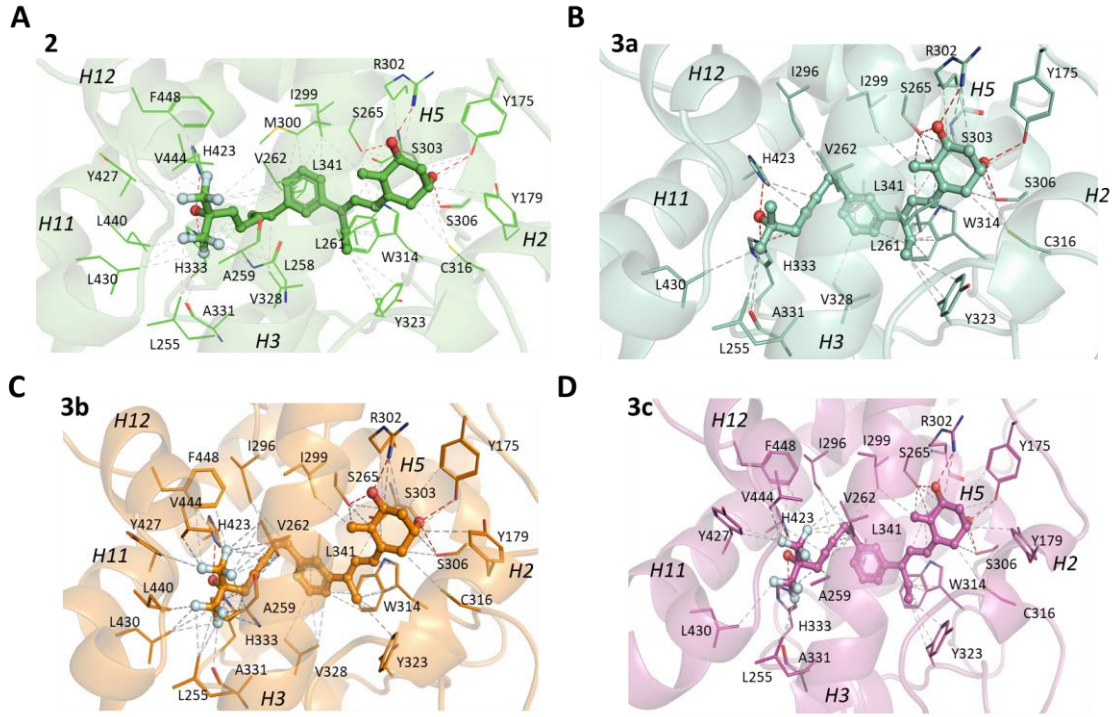

Figure 7. Interactions of des-C-ring and aromatic-D-ring analogs with zVDR LBD. (**A-D**) Interactions of **2** (**A**), **3a** (**B**), **3b** (**C**) and **3c** (**D**) with VDR residues within a 4 Å distance. Helices are labelled.

Thus, these structural data indicate that the four new analogs efficiently stabilize VDR agonistic conformation and that the compounds with fluorine atoms at the side chain terminus form the strongest interactions in agreement with their biological activities.

CONCLUSION

The new des-C-ring and aromatic-D-ring analogs, **2** and **3a-c,** which are characterized by a rigidified alkyne side chain or hexafluorine methyl groups were synthesized by the Wittig-Horner approach in 13 steps starting from commercial 3-bromobenzaldehyde [**2**

(22%); **3a** (26%); **3b** (21%); **3c** (24%)]. Binding assay confirmed the docking data showing that the compounds bind to VDR with similar affinity than the natural hormone 1,25D_3. Structural analysis confirmed that the compounds mimic the conformation of 1,25D_3 and maintain the hydrophobic interactions of 1,25D_3 as well as the important anchoring hydrogen bonds. In addition, they form specific interactions that efficiently stabilize VDR agonistic conformation. Interestingly, the new analogs lack hypercalcemic activity, but induce higher antiproliferative and transcriptional activity in breast cancer cells than 1,25D_3. More interestingly, the four compounds significantly decreased cell proliferation of TNBC cells when combined with cisplatin. These specific properties suggest a therapeutic potential of these compounds for the treatment of breast tumors.

EXPERIMENTAL SECTION

Docking procedure. Compounds structures as MOL2 files were generated with Chem3D. The ligands were energy minimized using the Chem3D MM2 Energy minimization tool, running the calculation to a minimum RMS gradient of 0.010 in vacuum at 300 K. Correct stereochemistry of the ligands after minimization was controlled. The crystal structure of 1,25D, obtained from the complex of 1,25D_3-hVDR (PDB 1DB1)[32] was used as reference ligand. Docking studies to predict the affinity of the new ligand for the VDR were carried out using the AutoDOCK VINA program (version 1.2.0).[31] The protein structure was extracted from PDB 1DB1 and not energy minimized. Coordinates for docking were assigned using AutoDOCK tools and were set to x = 10.19, y = 24.691 and z = 37.89. The size of the docking space was set to x = 26 Å and y,z =24 Å. The exhaustiveness was set to 60 and verbosity to 1. Docking parameters were set to default. Random seed was used to randomize the starting position of the ligand. The best 3 solutions were ranked with an associated score. Docking poses were visualized and structural figures were prepared using PyMOL.

Molecular Dynamics. The highest scoring docking pose of each ligand was taken as complex with 1,25D_3-hVDR (PDB 1DB1) and stored as pdb file. Molecular Dynamics calculations were performed as previously described using YASARA Suite.[33-34] Simulation was run for 20 ns with a simulation substep of 1.25 fs and simulation step of 2.5 fs.

Synthesis. General experimental procedures.[25] The purity of the final compounds (**2**, **3a**, **3b**, and **3c**) was assessed by HPLC phenomenex column [Luna 5 μ silica(2) 250 × 10

mm, normal phase, isocratic mode; 10-20% *i*-PrOH/hexanes; flow rate = 3 mL/min], and was identified as >95% (Supporting Information).

Ethyl (*E*)-3-(3-formylphenyl)acrylate (10). Palladium acetate (240 mg, 1.08 mmol, 0.02 equiv), triphenylphosphine (566 mg, 2.16 mmol, 0.04 equiv), ethyl acrylate (7.2 mL, 67.5 mmol, 1.25 equiv) and triethylamine (15 mL, 108.08 mmol, 2 equiv) were successively added to a solution of 3-bromobenzaldehyde (**7**, 10 g, 54.00 mmol, 1 equiv) in DMF (170 mL). The system was deoxygenated with argon. The mixture was heated to 125 °C for 19 h and then cooled to 23 ºC. The mixture was poured into water (250 mL) and extracted with Et_2O. The combined organic layers were washed with aqueous HCl (4N) and sat NaCl, dried and filtered. The filtrate was concentrated under reduced pressure to give ester **10** (10.5 g, 95%),[42] which was used in the next experiment without further purification.

Ethyl (*E*)-3-(3-(1-hydroxypropyl)phenyl)acrylate (**11a**). A solution of EtMgBr in THF (12.2 mL, 34.22 mmol, 2.8 M, 1.4 equiv) was added dropwise to a -78 ºC cooled solution of **10** (5 g, 24.44 mmol, 1 equiv) in dry THF (50 mL). The reaction mixture was stirred at −78 ºC for 1 h. The reaction was quenched by dropwise addition of saturated NH_4Cl (5 mL). The mixture was extracted with Et_2O (3 x 10 mL). The combined organic fractions were dried and concentrated. The residue was purified by flash chromatography (10% EtOAc/hexanes) to give alcohol **11a** [4.67 g, 82% R_f = 0.5 (30% EtOAc/hexanes)]. **^{1}H NMR** (250 MHz, $CDCl_3$): δ 7.64 (d, *J* =16.0, 1H), 7.33 (m, 4H), 6.38 (d, *J* = 16.0, 1H), 4.55 (t, *J* = 6.5, 1H), 4.18 (q, *J* = 7.1, 1H), 2.44 (br s, 1H), 1.73 (m, 2H), 1.28 (t, *J* = 7.1, 3H), 0.87 (t, *J* = 7.4, 3H). **^{13}C NMR** (63 MHz, $CDCl_3$): δ 167.1 (C=O), 145. 4 (=C), 144.3 (Car), 134.1 (Car), 128.6 (Car), 127.8 (Car), 126.9 (Car), 125.5 (Car), 118.2 (=C), 75.4 (C-O), 60.4 (CH_2), 31.6 (CH_2), 14.2 (CH_3), 9.9 (CH_3). **IR** (film, cm^{-1}): 3496, 2948, 2889, 1740, 1240. **HRMS** [ESI-TOF]$^+$, m/z) $[M+H]^+$ calcd for $C_{14}H_{18}O_3Na$, 257.1154; found 257.1148.

Ethyl 3-(3-(1-hydroxypropyl)phenyl)propanoate (**12a**). Pd/C (10%, 100 mg) was added to a solution of **11a** (1 g, 4.89 mmol, 1 equiv) in CH_2Cl_2 (30 mL). The mixture was evacuated and refilled with hydrogen three times and then stirred for 2.30 h under hydrogen atmosphere (balloon pressure). The mixture was filtered through a short pad of silica gel and washed with 20% EtOAc/hexanes. After concentration, the residue was purified by flash chromatography (20% EtOAc/hexanes) to give **12a** [1 g, 91%, R_f = 0.6 (30% EtOAc/hexanes), colorless oil]. **^{1}H NMR** (250 MHz, $CDCl_3$): δ 7.29 (m, 4H), 4.63

(t, J = 6.6, 1H), 4.19 (q, J = 7.1, 2H), 2.91 (t, J = 7.8, 1H), 2.69 (t, J = 7.4, 1H), 2.52 (br s, 1H) 1.83 (m, 2H), 1.31 (t, J = 7.1, 3H), 0.99 (t, J = 7.4, 3H). **^{13}C NMR (**63 MHz, $CDCl_3$): δ 172.8 (C=O), 144. 8 (Car), 140.5 (Car), 128.3 (Car), 127.2 (Car), 125.8 (Car), 123.8 (Car), 75.7 (C-O), 60.3 (CH_2), 35.8 (CH_2), 31.7 (CH_2), 30.8 (CH_2), 14.0 (CH_3), 10.0 (CH_3). **IR** (film, cm^{-1}): 3435, 2964, 2932, 2874, 1730, 1154. **HRMS** ([ESI-TOF]$^+$, m/z) $[M+H]^+$ calcd for $C_{14}H_{20}O_3Na$, 259.1304; found 259.1337.

Ethyl 3-(3-(1-((*tert*-butyldimethylsilyl)oxy)propyl)phenyl)propanoate (13a). Imidazole (1.5 g, 22.84 mmol, 2 equiv) and TBSCl (2.0 g, 13.71 mmol, 1.2 equiv) were successively added to a solution of alcohol **12a** (2.7 g, 11.42 mmol, 1 equiv) in dry DMF (30 mL). The reaction mixture was stirred for 12 h and then diluted with saturated NH4Cl (5 mL). The aqueous phase was extracted with hexanes (2 x 20 mL). The combined organic layers were dried, filtered and concentrated. The residue was purified by flash chromatography (hexanes) to afford **13a** [3.9 g, 98%, Rf = 0.80 (5% EtOAc/hexanes), colorless oil]. **^{1}H NMR** (250 MHz, $CDCl_3$): δ 7.25 (m, 4H), 4.67 (t, J = 6.1, 1H), 4.24 (q, J = 7.1, 2H), 3.07 (t, J = 7.8, 2H), 2.73 (t, J = 7.4, 1H), 1.78 (m, 2H) 1.35 (t, J = 7.1, 3H), 0.99 (m, 12H), 0.15 (s, 3H, MeSi), -0.01 (s, 3H, MeSi). **^{13}C NMR** (63 MHz, $CDCl_3$): δ 172.8 (C=O), 145. 8 (Car), 140.0 (Car), 127.9 (Car), 126.6 (Car), 125.6 (Car), 123.7 (Car), 76.2 (C-O), 60.2 (CH_2), 35.9 (CH_2), 33.5 (CH_2), 31.0 (CH_2), 25.7 (3xCH_3, Me_3CSi) 18.1 (C, CSi), 14.0 (CH_3), 9.9 (CH_3), -4.8 (CH_3, MeSi), -5.1 (CH_3, MeSi). **IR** (film, cm^{-1}): 2956, 2929, 2856, 1735, 1157. **HRMS** ([ESI-TOF]$^+$, m/z) $[M+H]^+$ calcd for $C_{20}H_{34}O_3NaSi$, 373.2169; found 373.2184.

3-(3-(1-((tert-Butyldimethylsilyl)oxy)propyl)phenyl)propanal (**14a**). A solution of Dibal-H in heptane (7.84 mL, 7.84 mmol, 1M, 1.1 equiv) was added dropwise to a at −78 ºC cooled solution of **13a** (2.5 g, 7.13 mmol, 1 equiv) in dry CH_2Cl_2 (50 mL). The reaction mixture was stirred at −78 ºC for 1 h, and at 23 ºC for 1 h. MeOH was carefully added and the mixture was stirred for 1 h. A solution of HCl (5%) was carefully added. The mixture was extracted with CH_2Cl_2 (3 x 30 mL). The combined organic fractions were dried, filtered and concentrated. The residue was purified by flash chromatography (2% EtOAc/hexanes) to afford **14a** [1.9 g, 87%, R$_f$ = 0.85 (5% EtOAc/hexanes), colorless oil]. **^{1}H NMR** (250 MHz, $CDCl_3$): δ 9.94 (t, J = 1.4, 1H), 7.29 (m, 4H), 4.67 (m, 1H), 3.07(dd, J_1 = 9.3, J_2 = 5.1, 2H), 2.90 (m, 2H), 1.78 (m, 2H), 1.0 (m, 12H, Me_3CSi, CH_3), 0.15 (s, 3H, MeSi), -0.01 (s, 3H, MeSi). **^{13}C NMR** (63 MHz, $CDCl_3$): δ 201.7 (C=O),

146. 0 (Car), 139.8 (Car), 128.0 (Car), 126.6 (Car), 125.6 (Car), 123.8 (Car), 76.0 (C-O), 45.2 (CH_2), 33.6 (CH_2), 28.1 (CH_2), 25.7 (3xCH_3, Me_3CSi), 18.2 (C, CSi), 10.0 (CH_3) -4.8 (C, CH_3, MeSi), -5.1(C, CH_3, MeSi). **IR** (film, cm^{-1}): 2955, 2928, 2856, 1727, 1083. **HRMS** ([ESI-TOF]$^+$, m/z) [M+H]$^+$ calcd for $C_{18}H_{30}O_2NaSi$, 329.1907; found 329.1926

1-(3-(4,4-Dibromobut-3-en-1-yl)phenyl)propan-1-ol *tert*-Butydimethylsilyl ether (15a). CBr_4 (6.2 g, 18.6 mmol, 3 equiv) was added to a suspension of PPh_3 (4.9 g, 18.6 mmol, 3 equiv) and Zn (1.2 g, 18.6 mmol, 3 equiv) in dry CH_2Cl_2 (36 mL) at 0 ºC. After 5 min, the cooling bath was removed and the reaction mixture was stirred at 23 ºC for 2 h. The color changed from green to deep red. A solution of aldehyde **14a** (1.9 g, 6.2 mmol, 1 equiv) in dry CH_2Cl_2 (10 mL) was added *via* cannula. The reaction mixture was stirred at 23 ºC for 1 h, filtered through a pad of silica gel (hexanes-20% EtOAc/hexanes). After concentration, the residue was purified by flash chromatography (1% EtOAc/hexanes) to afford dibromide **15a** [2.5 g, 87%), colorless oil, R_f = 0.70 (10% EtOAc/ hexanes). **^{1}H NMR** (250 MHz, $CDCl_3$): δ 7.14 (m, 4H), 6.37 (t, J = 7.2, 1H), 4.54 (t, J = 6.1, 1H), 2.71 (t, J = 7.6, 2H), 2.40 (m, 2H), 1.65 (m, 2H), 0.86 (m, 12H, 3xMe_3CSi, 3H CH_3), 0.02 (s, 3H, MeSi), -0.14 (s, 3H, MeSi). **^{13}C NMR** (63 MHz, $CDCl_3$): δ 146. 0 (Car), 140.0 (Car), 137.6 (C=C), 128.0 (Car), 126.7 (Car), 125.9 (Car), 123.9 (Car), 89.3 (C=C), 76.2 (C-O), 34.7 (CH_2), 33.9 (CH_2), 33.7 (CH_2), 25.7 (3xCH_3, Me_3CSi) 18.1 (C, CSi), 10.0 (CH_3), -4.6 (CH_3, MeSi), -4.9 (CH_3, MeSi). **IR** (film, cm^{-1}): 2955, 2927, 2855, 1607, 938. **HRMS** ([ESI-TOF]$^+$, m/z) [M+H]$^+$ calcd for $C_{13}H_{29}OSiBr_2$, 459.0349; found 459.0329

1-(3-(But-3-yn-1-yl)phenyl)propan-1-ol *tert*-Butyldimethylsilyl ether (6a). A solution of *n*-BuLi in hexanes (24 mL, 32.44 mmol, 1.35 M, 2.5 equiv) was slowly added to a -78 ºC cooled solution of dibromide **15a** (6 g, 12.98 mmol, 1 equiv) in dry THF (78 mL). The mixture was stirred at 0 ºC for 1 h. The reaction was quenched by addition of saturated NH_4Cl (15 mL). The mixture was extracted with TBDME (3 x 30 mL). The combined organic fractions were dried and concentrated. The residue was purified by flash chromatography (2% EtOAc/hexanes) to afford **6a** [3.9 g, 94%, R_f= 0.5 100% hexanes), colorless oil. **^{1}H NMR** (250 MHz, $CDCl_3$): δ 7.15 (m, 4H), 4.53 (t, J = 7.2, 1H), 2.80 (t, J = 6.1, 1H), 2.45 (m, 2H), 1.94 (t, J = 2.6, 2H), 1.64 (m, 2H), 0.86 (m, 12H, 3xMe_3CSi, 3H CH_3), 0.01 (s, 3H, MeSi), -0.15 (s, 3H, MeSi).**^{13}C NMR** (63 MHz, $CDCl_3$): δ 145. 8 (Car), 140.0 (Car), 127.9 (Car), 126.7 (Car), 126.0 (Car), 124.0 (Car), 83.8 (C≡C), 76.2 (C-O), 68.7 (C≡C), 34.9 (CH_2), 33.6 (CH_2), 25.7 (3xCH_3, Me_3CSi), 20.6 (CH_2), 18.1

(C, CSi), 10.0 (CH_3), -4.6 (CH_3, MeSi), -4.9 (CH_3, MeSi). **IR** (film, cm^{-1}): 3312, 2956, 2928, 2856, 2119. **HRMS** ([ESI-TOF]$^+$, m/z) [M+H]$^+$ calcd for $C_{19}H_{30}ONaSi$, 325.1958; found 325.1924.

7-(3-(1-((tert-Butyldimethylsilyl)oxy)propyl)phenyl)-2-methylhept-4-yn-2-ol (**9a**).
A solution of *n*-HexLi in THF (2.6 mL, 5.27 mmol, 2M, 1.5 equiv) was slowly added to a -78 ºC cooled solution of alkyne **6a** (1.12 g, 3.51 mmol, 1 equiv) in dry THF (23mL). The reaction mixture was stirred at −78 ºC for 1 h. The epoxide (0.62mL, 7.02 mmol, 2 equiv) and the $BF_3.OEt_2$ (0.86 mL, 7.02 mmol, 2 equiv) were successively added. The reaction mixture was stirred a at 23 ºC overnight. The reaction was quenched with of satd NH_4Cl (10mL). The mixture was extracted with TBDME (3 x 10 mL). The combined organic fractions were dried, filtered and concentrated. The residue was purified by flash chromatography (5% EtOAc/hexanes) to afford **9a** [1.28 g, 97%, R_f = 0.45 (5% EtOAc/hexanes), colorless oil]. **^{1}H NMR** (250 MHz, $CDCl_3$): δ 7.28 (m, 4H), 4.67 (t, *J* = 6.1, 1H), 2.92 (m, 2H, CH_2-Ph), 2.61 (m, 2H), 2.39 (t, *J* = 2.6, 2H, CH_2), 2.02 (b s, 1H, OH), 1.78 (m, 2H, CH_2CH_3), 1.34 (s, 6H, 2xCH_3), 0.98 (m, 12H, 3xMe_3CSi, 3H-CH_3), 0.14 (s, 3H, MeSi), -0.12 (s, 3H, MeSi). **^{13}C NMR** (63 MHz, $CDCl_3$): δ 145. 7 (Car), 140.1 (Car), 127.7 (Car), 126.6 (Car), 125.6 (Car), 123.7 (Car), 82.5 (C≡C), 76.4 (C-O), 70.8 (C≡C), 69.6 (C, C-OH), 35.2 (CH_2) 34.3 (CH_2), 33.5 (CH_2), 28.3 (C, 2xCH_3,), 25.7 (C, 3xCH_3, Me_3CSi), 20.6 (CH_2), 9.9 (CH_3), 18.1 (C, CSi), -4.7 (CH_3, MeSi), -5.1 (CH_3, MeSi). **IR** (film, cm^{-1}): 3410, 2955, 2944, 2877, 2150, 1092. **HRMS** ([ESI-TOF]$^+$, m/z) [M+H]$^+$ calcd for $C_{23}H_{38}O_2SiNa$, 397.2539; found 397.2535.

Same procedures were used for the preparation of 11b, 12b, 13b, 14b, 15b, 6b, 9b, and 9c.

11b [84%, R_f= 0.5 (30% EtOAc/hexanes)]. **^{1}H NMR** (250 MHz, $CDCl_3$): δ 7.64 (dd, J_1 = 16.0, J_2 = 3.4, 1H), 7.43 (m, 4H, $H_{ar,}$), 6.40 (dd, J_1 = 16.0, J_2 = 3.4, 1H), 4.86 (m, 1H), 4.21 (qd, J_1 = 7.1, J_2 = 3.0, 2H), 2.01 (br s, 1H), 1.46 (dd, J_1 = 6.5, J_2 = 3.0 Hz, 3H), 1.29 (td, J_1 = 7.1, J_2 = 2.3, 3H). **^{13}C NMR** (63 MHz, $CDCl_3$): δ 166.6 (C=O), 146.3 (Car), 144.3 (Car), 134.1 (Car), 128.6 (Car), 127.1 (Car), 126.96 (Car) 124.8 (Car), 118.2 (=C), 69.6 (C-O), 60.3 (CH_2), 25.2 (CH_3), 14.1 (CH_3). **IR** (film, cm^{-1}): 3495, 2946, 2915, 1654, 1593, 1205. **HRMS** ([ESI-TOF]$^+$, m/z) [M+H]$^+$ calcd for $C_{13}H_{16}O_3Na$, 243.0997; found 259.0992.

12b [90%, R_f = 0.57 (30% EtOAc/hexanes), colorless oil]. **^{1}H NMR** (250 MHz, $CDCl_3$): δ 7.17 (m, 4H, $H_{ar,}$), 4.83 (q, *J* = 6.4, 1H), 4.08 (q, *J* = 7.1, 2H), 2.91 (t, *J* = 7.8, 2H), 2.58 (t, *J* = 7.8, 2H), 2.01 (br s, 1H), 1.44 (d, *J* = 6.4, 3H), 1.20 (t, *J* = 7.1 3H). **^{13}C NMR** (63 MHz, $CDCl_3$): δ 173.1 (C=O), 145.9 (Car), 140.3 (Car), 128.4 (Car), 126.8 (Car), 125.2 (Car), 123.5 (=C), 70.1 (C-O), 60.3 (CH_2), 35.7 (CH_2), 30.8 (CH_2), 25.0 (CH_3). 14.0 (CH_3). **IR** (film, cm^{-1}): 3414, 2975, 2930, 2871, 1727, 1157. **HRMS** $[ESI\text{-}TOF]^+$, m/z) $[M+H]^+$ calcd for $C_{13}H_{18}O_3Na$, 245.1148; found 245.1182.

13b [96%, R_f = 0.80 (5% EtOAc/hexanes), colorless oil]. **^{1}H NMR** (250 MHz, $CDCl_3$): δ 7.16 (m, 4H), 4.82 (q, *J* = 6.3, 1H), 4.11 (q, *J* = 7.1, 2H), 2.93 (t, *J* = 7.6, 2H), 2.59 (t, *J* = 7.4, 2H), 1.38 (d, *J* = 6.3, 3H), 1.21(t, *J* = 7.1, 3H), 0.89 (s, 9H, Me_3CS), 0.03 (s, 3H, MeSi), -0.05 (s, 3H, MeSi). **^{13}C NMR** (63 MHz, $CDCl_3$): δ 172.7 (C=O), 147.0 (Car), 140.1 (Car), 128.0 (Car), 126.5 (Car), 125.0 (Car), 123.0 (Car), 70.6 (C-O), 60.1 (CH_2), 35.8 (CH_2), 30.9 (CH_2), 27.1 (CH_3), 25.7 (3xCH_3, Me_3CSi) 18.1 (C, CSi), 14.1 (CH_3), -4.9 (CH_3, MeSi), -5.0 (CH_3, MeSi). **IR** (film, cm^{-1}): 2955, 2928, 2856, 1735, 1160. **HRMS** $[ESI\text{-}TOF]^+$, m/z) $[M+H]^+$ calcd for $C_{19}H_{32}O_3NaSi$, 359.2012; found 359.2042.

14b [90%, R_f = 0.50 (2% EtOAc/hexanes), colorless oil]. **^{1}H NMR** (250 MHz, $CDCl_3$): δ 9.91 (t, *J* = 1.4, 1H), 7.25 (m, 4H), 4.93 (q, *J* = 6.3, 1H), 3.02 (m, 2H), 2.86 (m, 2H), 1.48 (d, *J* = 6.4, 3H), 0.99 (s, 9H, Me_3CSi), 0.14 (s, 3H, MeSi), 0.06 (s, 3H, MeSi).**^{13}C NMR** (63 MHz, $CDCl_3$): δ 201.5 (C=O), 147. 2 (Car), 139.9 (Car), 128.5 (Car), 126.6 (Car), 125.0 (Car), 123.2 (Car), 70.7 (C-O), 45.2 (CH_2), 28.4 (C, CSi), 27.1 (CH_2), 25.7 (3xCH_3, Me_3CSi) 18.1 (C, CH_3), -4.8 (2XCH_3, MeSi). **IR** (film, cm^{-1}): 2954, 2928, 2856, 1710, 1161. **HRMS** $[ESI\text{-}TOF]^+$, m/z) $[M+H]^+$ calcd for $C_{17}H_{28}O_2NaSi$, 315.175; found 315.1769.

15b [89%, colorless oil, R_f = 0.70 (5% EtOAc/ hexanes)]. **^{1}H NMR** (250 MHz, $CDCl_3$): δ 7.19 (m, 4H), 6.39 (t, *J* = 7.2, 1H), 4.84 (q, *J* = 6.3, 1H), 2.71 (t, *J* = 7.7, 2H), 2.38 (m, 2H), 1.39 (d, *J* = 6.3, 3H), 0.89 (s, 9H, Me_3CSi), 0.04 (s, 3H, MeSi), -0.04 (s, 3H, MeSi). **^{13}C NMR** (63 MHz, $CDCl_3$): δ 147. 0 (Car), 140.1 (Car), 137.5 (C=C), 128.0 (Car), 126.5 (Car), 125.0 (Car), 123.0 (Car), 89.2 (C=C), 70.6 (C-O), 34.5 (CH_2), 33.7 (CH_2), 27.1 (CH_3), 25.7 (3xCH_3, Me_3CSi) 18.1 (C, CSi), -4.9 (2XCH_3, MeSi). **IR** (film, cm^{-1}): 2953, 2927, 2855, 1607, 969. **HRMS** $[ESI\text{-}TOF]^+$, m/z) $[M+H]^+$ calcd for $C_{18}H_{28}ONaSiBr_2$, 469.0168; found 469.0177

6b [94%, R_f = 0.5 (100% hexanes), colorless oil]. **^{1}H NMR** (250 MHz, $CDCl_3$): δ 7.24 (m, 4H), 4.92 (q, *J* = 6.3, 1H), 2.91 (t, *J* = 7.6, 2H), 2.54 (td, J_1 = 7.5, J_2 = 2.5, 2H), 2.03 (t, *J* =2.5, 1H), 1.47 (d, *J* = 6.3, 3H), 0.97 (s, 9H, Me_3CSi), 0.12 (s, 3H, MeSi), 0.04 (s, 3H, MeSi).**^{13}C NMR** (63 MHz, $CDCl_3$): δ 147. 2 (Car), 140.0 (Car), 128.1 (Car), 126.6 (Car), 125.2 (Car), 123.2 (Car), 83.8 (C≡C), 70.9 (C-O), 68.7 (C≡C), 34.9 (CH_2), 27.2 (CH_2), 25.7 (3xCH_3, Me_3CSi), 20.4 (CH_3), 18.1 (C, CSi), -4.9 (2XCH_3, MeSi).**IR** (film, cm^{-1}): 3310, 2954, 2925, 2856, 2119. HRMS ([ESI-TOF]$^+$, m/z) [M+H]$^+$ calcd for $C_{18}H_{28}ONaSi$; 311.1807 found 311.1814.

(9b) [0.57 g, 90%, R_f = 0.45 (5% EtOAc/hexanes), colorless oil. **^{1}H NMR** (250 MHz, $CDCl_3$): δ 7.15 (m, 4H), 4.55 (t, *J* = 6.1, 1H), 3.30 (s, 1H, OH), 2.81 (m, 4H), 2.52 (td, J_1 = 7.5, J_2 = 2.5, 2H), 1.66 (m, 2H), 0.88 (m, 12H), 0.02 (s, 3H, MeSi), 0.014 (s, 3H, MeSi). **^{13}C NMR** (63 MHz, $CDCl_3$): δ 146. 0 (Car), 139.5 (Car), 127.9 (Car), 126.5 (Car), 125.6 (Car), 124.4 (C-F), 124.1(Car), 120.0 (C-F), 87.1 (C≡C), 77.0 (C-2CF_3), 76.0 (C-O), 69.5 (C≡C), 34.4 (CH_2), 33.5 (CH_2), 25.7 (3xCH_3, Me_3CSi), 22.1 (CH_2), 20.5 (CH_2), 18.1 (C, CSi), 9.8 (CH_3) -4.9 (CH_3, MeSi), -5.2 (CH_3, MeSi). **IR** (film, cm^{-1}): 3493, 2955, 2945, 2876, 1214. **HRMS** ([ESI-TOF]$^+$, m/z) [M+H]$^+$ calcd for $C_{23}H_{32}O_2F_6SiNa$, 505.1973; found 505.1965.

9c [0.74 g, 91%, R_f = 0.45 (5% EtOAc/hexanes), colorless oil. **^{1}H NMR** (250 MHz, $CDCl_3$): δ 7.17 (m, 4H), 4.85 (q, *J* = 6.3, 1H, CHOTBS), 3.34 (br s, 1H, OH) 2.82 (m, 4H), 2.52 (td, J_1 = 7.5, J_2 = 2.5, 2H), 1.39 (d, *J* = 6.4 3H, CH_3CHOTBS), 0.90 (s, 9H, Me_3CSi), 0.04 (s, 3H, MeSi), -0.04 (s, 3H, MeSi). **^{13}C NMR** (63 MHz, $CDCl_3$): δ 147. 2 (Car), 139.6 (Car), 128.1 (Car), 126.4 (Car), 124.9 (Car), 124.6 (C-F), 123.3 (Car),120.0 (C-F), 87.1 (C≡C), 77.3 (C-2CF_3), 70.5 (C-O), 69.6 (C≡C), 34.4 (CH_2), 27.0 (CH_3), 25.7 (3xCH_3, Me_3CSi), 22.1 (CH_2), 20.4 (CH_2),18.1 (C, CSi), -5.05 (2XCH_3, MeSi). **IR** (film, cm^{-1}): 3493, 2955, 2930, 2858, 1203, 1203. **HRMS** ([ESI-TOF]$^+$, m/z) [M+H]$^+$ calcd for $C_{22}H_{31}O_2F_6Si$, 469.19920; found 469.19965.

7-(3-(1-((*tert*-Butyldimethylsilyl)oxy)propyl)phenyl)-1,1,1-trifluoro-2-(trifluoromethyl)heptan-2-ol (17a). PtO_2 (60 mg of 10%) was added to a solution of **9b** (0.2 g, 0.414 mmol, 1 equiv) in THF (10 mL). The mixture was evacuated and refilled with hydrogen for three times and then stirred for 2 h under hydrogen atmosphere (balloon pressure). The mixture was filtered through a short pad of celite and washed with 20%

EtOAc/hexanes. After concentration, the residue was purified by flash chromatography (20% EtOAc/hexanes) to give **17a** [0.197 g, 98%, R_f = 0.55 (10% EtOAc/hexanes), colorless oil]. **^{1}H NMR** (250 MHz, $CDCl_3$): δ 7.12 (m, 4H), 4.55 (t, *J* = 6.1, 1H), 3.43 (s, 1H, OH), 2.61 (t, *J* = 7.5, 2H), 1.88 (m, 2H), 1.61 (m, 6H), 1.35 (m, 2H), 0.88 (m, 12H), 0.03 (s, 3H, MeSi), -0.013 (s, 3H, MeSi).**^{13}C NMR** (63 MHz, $CDCl_3$): δ 145.6 (Car), 141.7 (Car), 127.7 (Car), 126.7 (Car), 125.8 (Car), 125.4 (C-F), 123.3 (Car), 120.0 (C-F), 76.9 (C-2CF_3), 76.2 (C-O), 35.6 (CH_2), 33.6 (CH_2), 30.8 (CH_2), 30.3 (CH_2), 29.2 (CH_2), 25.7 (3xCH_3, Me_3CSi), 25.3 (CH_2), 21.5 (CH_2), 18.1 (C, CSi), 10.0 (CH_3) -4.9 (CH_3, MeSi), -5.1 (CH_3, MeSi). **IR** (film, cm^{-1}): 3488, 2955, 2945, 2876, 1209, 1200. **HRMS** ([ESI-TOF]$^+$, m/z) $[M+H]^+$ calcd for $C_{23}H_{36}O_2F_6SiNa$, 509.2286; found 509.2281.

1,1,1-Trifluoro-7-(3-(1-hydroxypropyl)phenyl)-2-(trifluoromethyl)heptan-2-ol (17b). A solution of *n*-Bu_4NF in THF (0.70 mL, 0.70 mmol, 1M, 1.5 equiv) was added to a solution of **17a** (0.23 g, 0.47 mmol, 1 equiv) in dry THF (10 mL). The mixture was stirred at 23 ºC for 12 h and then diluted with saturated NH_4Cl (5 mL). The mixture was extracted with EtOAc (3 x 10 mL). The combined organic fractions were dried, filtered and concentrated. The residue was purified by flash chromatography (30% EtOAc/hexanes) to afford **17b** [0.174 g, 99%, R_f = 0.50 (30% EtOAc/hexanes), colorless oil]. **^{1}H NMR** (250 MHz, $CDCl_3$): δ 7.13 (m, 4H), 4.53 (t, *J* = 6.6, 1H), 4.15 (s, 1H, OH), 2.60 (t, *J* = 7.6, 2H), 2.19 (s, 1H, OH), 1.75 (m, 8H, (4xCH_2), 1.33 (dd, J_1 = 14.9, J_2 = 8, 2H), 0.87 (t, *J* = 7.4, 1H). **^{13}C NMR** (63 MHz, $CDCl_3$): δ 144.0 (Car), 142.4 (Car), 128.2 (Car), 127.5 (Car), 125.9 (Car), 125.4 (C-F), 123.4 (Car), 120.9 (C-F), 76.2 (C-O), 35.5 (CH_2), 31.4 (CH_2), 30.7 (CH_2), 30.4 (CH_2), 29.3 (CH_2), 25.4 (CH_2), 21.4 (CH_2), 9.9 (CH_3). **IR** (film, cm^{-1}): 3489, 3011, 2961, 2877, 1208, 1184, 1112. **HRMS** ([ESI-TOF]$^+$, m/z) $[M+H]^+$ calcd for $C_{17}H_{22}O_2F_6Na$, 395.1259; found 325.1262.

1-(3-(7,7,7-Trifluoro-6-hydroxy-6-(trifluoromethyl)heptyl)phenyl)propan-1-one (5a). Dess-Martin periodinane (DMP) (0.140 g, 0.33 mmol, 1.1 equiv) was added to a solution of diol **17b** (0.112 g, 0.30 mmol, 1 equiv) in dry CH_2Cl_2 (5 mL). The mixture was stirred at 23 ºC for 40 min. The reaction was quenched with saturated NaCl (4 mL). The mixture was extracted with CH_2Cl_2 (3 x 10 mL). The combined organic fractions were dried, filtered and concentrated. The residue was purified by flash chromatography (15% EtOAc/hexanes) to afford **5a** [0.108 g, 97 %, R_f = 0.55 (20% EtOAc/hexanes), colorless oil]. **^{1}H NMR** (250 MHz, $CDCl_3$): δ 7.76 (m, 2H), 7.36 (m, 2H), 4.42 (br s, 1H,

OH), 3.00 (q, J = 7.3, 2H), 2.66 (t, J = 7.6, 2H), 1.92 (m, 2H), 1.63 (m, 4H), 1.38 (m, 2H), 1.21 (t, J = 7.3, 3H). **^{13}C NMR** (63 MHz, $CDCl_3$): δ 202.0 (C=O), 142.7 (Car), 136.7 (C-F), 133.1 (Car), 128.4 (Car), 127.7 (Car), 125.6 (C-F), 125.5 (Car), 120.9 (C-F), 76.0 (C-2CF_3), 35.4 (CH_2), 33.5 (CH_2), 31.7 (CH_2), 30.7 (CH_2), 30.4 (CH_2), 29.5 (CH_2), 25.2 (CH_2), 21.5 (CH_2), 8.1 (CH_3). **IR** (film, cm^{-1}): 3378, 3010, 2884, 1675, 1205. **HRMS** ([ESI-TOF]$^+$, m/z) $[M+H]^+$ calcd for $C_{17}H_{20}O_2F_6Na$, 393.1265; found 393.1260.

1-(3-(7,7,7-trifluoro-6-((triethylsilyl)oxy)-6-(trifluoromethyl)heptyl)phenyl)propan-1-one (5b). Imidazole (36.7 mg, 0.54 mmol, 2 equiv), DMAP (6.9 mg, 0.54 mmol, 0.2 equiv) and triethylsilyl chloride (TESCl) (0.092 mL, 0.54 mmol, 2 equiv) were successively added to a solution of alcohol **5a** (0.100 g, 0.27 mmol, 1 equiv). The reaction was quenched with (5 mL) of H_2O. The mixture was extracted with TBDME (3 x 10 mL). The organic fractions were dried, filtered and concentrated. The residue was purified by flash chromatography (15% EtOAC/hexanes) to afford **5b**. [0.120g, 97%, R_f = 0.55 (20% EtOAc/hexanes), colorless oil]. **^{1}H NMR** (250 MHz, $CDCl_3$): δ 7.74 (m, 2H), 7.33 (m, 2H), 2.97 (t, J = 7.3, 2H), 2.64 (t, J = 7.6, 2H), 1.90 (m, 2H), 1.61 (m, 4H), 1.38 (m, 2H), 1.19 (t, J = 7.3, 3H, CH_3-Et), 0.94 (t, J = 7.9, 9H, 3x(CH_3CH_2)Si), 0.90 (q, J = 7.9, 6H, 3xCH_2Si). **^{13}C NMR** (63 MHz, $CDCl_3$): δ 201.7 (C=O), 142.7 (Car), 136.7 (C-ar), 133.0 (Car), 128.4 (Car), 127.7 (Car), 125.5 (Car), 121.0 (C-F), 76.3 (C-2CF_3), 35.4 (CH_2), 31.7 (CH_2), 30.7 (CH_2), 30.5 (CH_2), 29.3 (CH_2), 21.5 (CH_2), 8.1 (CH_3), 6.3 (CH_3), 5.5 (CH_2). **IR** (film, cm^{-1}): 2954, 2932, 2875, 1673, 1215. **HRMS** ([ESI-TOF]$^+$, m/z) $[M+H]^+$ calcd for $C_{23}H_{34}O_2F_6SiNa$, 507.2130; found 507.2124.

(1*R*,3*S*,*Z*)-4-Methylene-5-((*E*)-3-(3-(7,7,7-trifluoro-6-hydroxy-6 (trifluoromethyl) heptyl)phenyl) pent-2-en-1-ylidene)cyclohexane-1,3-diol (2). A solution of *n*-butyllithium in hexane (0.38 mL, 0.911 mmol, 2.36 M, 4.8 equiv) was added dropwise to a -78 °C cooled solution of phosphine oxide **4a** (0.53 g, 0.911 mmol, 4.8 equiv) in THF (5 mL). The resulting red solution of the anion **4b** was stirred at the same temperature for 30 min. A solution of ketone **5b** (92 mg, 0.190 mmol, 1 equiv) in dry THF (2.5 mL) was added dropwise. The resulting solution was stirred at -78 °C for 90 min. The became pale orange solution was allowed to reach 23 ºC (2 h). A drop of H_2O was added, and the solvents were removed in vacuo. The residue was dissolved in EtOAc/hexanes, washed with a sat $NaHCO_3$, sat NaCl, filtered, dried and concentrated in vacuo. Removal of

solvents in vacuo afforded a residue which was flash chromatographed (50% EtOAc/ hexanes) to afford a mixture of the protected **2** and its (7*Z*)-isomer (ratio, 4:1) [0.110 g, 0.129 mmol, 68%], which was dissolved in THF (5 mL). A solution of TBAF (0.77 mL, 0.77 mmol, 1 M, 6 equiv) was added. The mixture was stirred at 23 ºC for 24 h in the dark. The reaction was quenched with sat NH_4Cl (4 mL) and the mixture was extracted with EtOAc (2 x 5 mL). The combined organic layers were dried, filtered and concentrated. The residue was flash chromatographed (SiO_2, 50% EtOAc/hexanes) and HPLC purified (Phenomenex SiO_2, Luna Silica(2) 5µ, 250 x 10 mm, 10% *i*-PrOH/hexanes) to affford pure **2** [53 mg, 0.104 mmol, 55%, two steps, R_f = 0.38 (50% EtOAc/hexanes],white foam. $[\alpha]_D^{25}$ = +16.8° (c = 5 in EtOH). UV (96% EtOH): λ_{max}: 300 nm (ε= 14.105), λ_{min} = 254 nm]. **^{1}H NMR** (250 MHz, $CDCl_3$): δ 7.19 (m, 3H), 7.02 (m, 1H), 6.62 (d, *J* = 11.4, 1H, H-7), 6.41 (d, *J* = 11.4, 1H, H-6), 5.32 (s, 1H,H-19), 5.03 (s, 1H, H-19), 4.43 (t, *J* = 5.4, 1H, H-1), 4.21(m,1H, H-3), 4.05 (br s, 1H, OH), 2.61 (m, 5H), 2.35 (dd, J_1 = 16.1 J_2 = 7.9, 1H), 1.9 (m, 6H), 1.62 (m, 5H), 1.36 (m, 2H), 1.03 (t, *J* = 7.4, 3H, Me).**^{13}C NMR** (63 MHz,$CDCl_3$): δ 147.0 (=C), 143.1 (=C), 142.3 (=C), 142.0 (=CH), 136.3 (=C), 128.1 (C-F), 126.9 (CH), 126.2 (C-F), 125.5 (CH), 123.5 (CH), 122.9 (CH), 113.0 (CH_2, C-19), 77.1 (C, COH), 71.0 (CH, C-1), 66.7 (CH, C-3), 45.2 (CH_2), 42.6 (CH_2), 35.4 (CH_2), 30.7 (CH_2), 30.6 (CH_2), 29.1 (CH_2), 22.9 (CH_2), 21.5 (CH_2), 13.8 (CH_3). **IR** (film, cm^{-1}): 3365, 3009, 2932, 2882, 1376, 1215. **HRMS** ([ESI-TOF]$^+$, m/z) $[M+H]^+$ calcd for $C_{26}H_{32}O_3F_6Na$, 529.2153; found 529.2151.

7-(3-(1-Hydroxypropyl)phenyl)-2-methylhept-4-yn-2-ol (18a). A solution of *n*-Bu_4NF in THF (4.4 mL, 4.40 mmol, 1M, 1.5 equiv) was added to a solution of **9a** (1.1 g, 2.93 mmol, 1 equiv) in dry THF (28 mL). The mixture was stirred at 23 ºC or 12 h and then diluted with saturated NH_4Cl (7 mL). The mixture was extracted with EtOAc (5 x 10 mL). The combined organic fractions were dried, filtered and concentrated. The residue was purified by flash chromatography (50% EtOAc/hexanes) to afford **18a** [0.74 g, 97%, R_f = 0.40 (50% EtOAc/hexanes), colorless oil]. **^{1}H NMR** (250 MHz, $CDCl_3$): δ 7.18 (m, 4H), 4.51 (t, *J* = 6.6, 1H), 2.78 (t, *J* = 7.0, 2H), 2.49 (m, 2H), 2.25 (b s, 2H, 2xOH), 2.2 (t, *J* = 2.1, 2H), 1.72 (m, 2H), 1.13 (s, 6H, 2XCH_3), 0.88 (t, *J* = 7.4, 3H). **^{13}C NMR** (63 MHz, $CDCl_3$): δ 144. 9 (Car), 140.7 (Car), 128.5 (Car), 127.4 (Car), 126.5 (Car), 124.2 (Car), 82.7 (C≡C), 76.5 (C-O), 69.7 (C≡C), 68.9 (C, C-OH), 34.9 (CH_2), 34.3 (CH_2), 31.6 (CH_2), 28.3 (2xCH_3,), 20.8 (CH_2), 10.1 (CH_3). **IR** (film, cm^{-1}): 3369,

2968, 2929, 2875, 1157. **HRMS** ([ESI-TOF]$^+$, m/z) [M+H]$^+$ calcd for $C_{17}H_{24}O_2Na$, 283.1668; found 283.1686.

1-(3-(6-Hydroxy-6-methylhept-3-yn-1-yl)phenyl)propan-1-one (**8a**). DMP (1.25 g, 2.95 mmol, 1.1 equiv) was added to a solution of alcohol **18a** (0.7 g, 2.68 mmol, 1 equiv) in dry CH_2Cl_2 (30 mL). The mixture was stirred at 23c ºC for 40 min. The reaction was quenched with H_2O (10 mL). The mixture was extracted with TBDME (3 x 10 mL). The combined organic fractions were dried, filtered and concentrated. The residue was purified by flash chromatography (15% EtOAc/hexanes) to afford **8a** [0.63 g, 91%, R_f = 0.55 (30% EtOAc/hexanes), colorless oil]. **^{1}H NMR** (250 MHz, $CDCl_3$): δ 7.76 (m, 2H), 7.36 (m, 2H), 2.95 (q, *J* = 7.0, 2H), 2.82 (t, *J* = 7.2, 2H), 2.48 (t, *J* = 7.1, 2H), 2.25 (s, 2H), 2.02 (b s, 1H, OH), 1.17 (m, 9H, 3XCH_3). **^{13}C NMR** (63 MHz, $CDCl_3$): δ 200.8 (C=O), 141.0 (Car), 137.0 (Car), 133.0 (Car), 128.4 (Car), 127.8 (Car), 126.0 (Car), 81.9 (C≡C), 77.7 (C≡C), 69.7 (C, C-OH), 34.8 (CH_2), 34.2 (CH_2), 31.7 (CH_2), 28.3 (C, 2xCH_3), 20.5 (CH_2), 8.1 (CH_3). **IR** (film, cm^{-1}): 3427, 2972, 2933, 2848, 2364, 1681, 1163. **HRMS** ([ESI-TOF]$^+$, m/z) [M+H]$^+$ calcd for $C_{17}H_{22}O_2Na$, 281.1512; found 281.1544.

1-(3-(6-Methyl-6-((triethylsilyl)oxy)hept-3-yn-1-yl)phenyl)propan-1-one (19a). Imidazole (68.0 mg, 0.54 mmol, 2 equiv) and triethylsilyl chloride (TESCl) (0.092 mL, 0.54mmol, 2 equiv) were successively added to a solution of alcohol **8a** (0.1 g, 0.27 mmol, 1 equiv) in dry DMF (4 mL). The mixture was stirred at 23 ºC for 12 h. The reaction was quenched with H_2O (5 mL). The mixture was extracted with TBDME (3 x 10 mL). The combined organic fractions were dried, filtered and concentrated. The residue was purified by flash chromatography (15% EtOAC/hexanes) to afford **19a**. [0.130 g, 99%, R_f = 0.60 (20% EtAc/hexanes), colorless oil]. **^{1}H NMR** (250 MHz, $CDCl_3$): δ 7.78 (m, 2H), 7.35 (m, 2H), 2.97 (m, 2H), 2.83 (t, *J* = 7.3, 2H), 2.47 (m, 2H), 2.24 (d, *J* = 2.0, 2H), 1.17 (m, 9H, CH_3Et, 2xCH_3COTES), 0.90 (m, 9H, 3xCH_3CH_2Si), 0.52 (m, 6H, 3xCH_2Si). **^{13}C NMR** (63 MHz, $CDCl_3$): δ 200.7 (C=O), 141.2 (Car), 136.8 (Car), 133.0 (Car), 128.3 (Car), 127.9 (Car), 125.8 (Car), 80.4 (C≡C), 78.9 (C≡C), 73.0 (C, COTES), 35.2 (CH_2), 35.1 (CH_2), 31.7 (CH_2), 29.1 (2xCH_3, 2xCH_3COH), 20.7 (CH_2), 8.1 (C, CH_3-Et), 6.9 (3xCH_3, 3xCH_3CH_2Si), 6.5 (3xCH_2, 3xCH_2Si). **IR** (film, cm^{-1}): 2954,

2910, 2875, 1688, 1239, 1046. **HRMS** ([ESI-TOF]$^+$, m/z) [M+H]$^+$ calcd for $C_{23}H_{36}O_2NaSi$, 395.2376; found 395.2377**.**

(1*R*,3*S*,*Z*)-5-((*E*)-3-(3-(6-Hydroxy-6-methylhept-3-yn-1-yl)phenyl)pent-2-en-1-ylidene)-4-methylenecyclohexane-1,3-diol (3a). A solution of *n*-butyllithium in hexanes (0.40 mL, 0.943 mmol, 2.34 M, 3.3 equiv) was added dropwise to a -78 °C cooled solution of phosphine oxide **4a** (0.55 g, 0.943 mmol, 3.3 equiv) in THF (5 mL). The resulting red solution of the resulting anion was stirred at the same temperature for 30 min. A solution of ketone **19a** (0.110 g, 0.29 mmol. 1 equiv) in dry THF (2.5 mL) was added dropwise. The resulting solution was stirred at -78 °C for 90 min. The pale orange mixture was allowed to come slowly to 23 ºC (2 h). A drop of H_2O was added, and the solvents were removed *in vacuo*. The residue was redissolved in EtOAc/hexanes, washed with a sat $NaHCO_3$, sat NaCl, filtered, dried and concentrated *in vacuo*. The residue was flash chromatographed on silica gel (50% EtOAc/ hexanes) to afford a mixture of the protected analog **3a** (77 mg, 0.1044 mmol) and its partially deprotected (-$SiEt_3$) compound (45 mg, 0.0722 mmol). Both reaction products contain the natural vitamin D triene system and its (7*Z*)-isomer [(7*E*/7*Z*, 4:1). The mixture was dissolved in THF (5 mL). A solution of TBAF (1.0 mL, 1.0 mmol, 1 M, 6 equiv) was added. The mixture was stirred at 23 ºC for 24 h in the dark. The reaction was quenched whit sat NH_4Cl (4 mL) and the mixture was extracted with EtOAc (2 x 5 mL). The combined organic layers were dried, filtered and concentrated *in vacuo*. The residue was flash chromatographed (SiO_2, 1.5 x 8 cm, 60% EtOAc/hexanes) and repurified by HPLC (Phenomenex SiO_2, Luna Silica(2) 5μ, 250 x 10 mm, 10% *i*-PrOH/hexanes) to afford pure **3a** [35 mg, 30% (two steps), R_f = 0.38 (50% EtOAc/hexanes), foam white]. $[\alpha]_D^{25}$ = +10.8° (c = 5 in EtOH). UV (96% EtOH): λmax: 298 nm (ε = 15344), λmin = 254 nm]. **^{1}H NMR** (250 MHz, $CDCl_3$): δ 7.21 (m, 3H), 7.07 (m, 1H), 6.62 (d, *J* = 11.4, 1H, H-7), 6.41 (d, *J* = 11.4, 1H, H-6), 5.32 (s, 1H, H-19), 5.02 (s, 1H, H-19), 4.43 (t, *J* = 5.4, 1H, H-1), 4.23 (m, 1H, H-3), 2.78 (t, *J* = 7.1 2H), 2.64 (m, 3H), 2.49 (m, 2H), 2.35 (dd, J_1 = 13.2, J_2= 7.4,1H), 2.26 (d, *J* = 2.1, 2H), 1.96 (m, 4H), 1.17 (s, 3H, CH_3COH), 1.15 (s, 3H, CH_3COH), 1.02 (t, *J* = 7.5, 3H, Me). **^{13}C NMR** (63 MHz,$CDCl_3$): δ 147.4 (=C), 142.5 (=C), 142.4 (=C), 140.4 (=CH), 136.9 (=C), 128.1 (CH), 126.8 (CH), 126.2 (CH), 125.1 (CH), 124.0 (CH), 123.0 (CH), 112.8 (CH_2, C-19), 82.44 (C≡), 76.8 (C, COH), 70.8 (CH, C-1), 69.6 (C≡),

66.5 (CH, C-3), 45.3 (CH_2), 42.5 (CH_2), 35.0 (CH_2), 34.2 (CH_2), 28.2 (CH_3), 28.1 (C), 25.1 (CH_2), 22.9 (CH_2), 20.5 (CH_2), 13.8(CH_3). **IR** (film, cm^{-1}): 3365, 2951, 2932, 2857, 1376. **HRMS** ([ESI-TOF]$^+$, m/z) $[M+H]^+$ calcd for $C_{26}H_{34}O_3Na$, 417.2406; found 417.2402.

Same procedures were used for the preparation of 18b, 18c, 8b, 8c, 19b, 19c, 3b, and 3c.

18b [0.286 g, 94%, R_f = 0.40 (50% EtOAc/hexanes), colorless oil]. **^{1}H NMR** (250 MHz, $CDCl_3$): δ 7.18 (m, 4H), 4.54 (t, *J* = 6.6, 1H, CHO), 2.79 (m, 4H), 2.51 (m, 2H), 1.75 (m, 2H), 1.23 (br s, 1H, OH) 0.88 (t, *J* = 7.4, 3H, Me). **^{13}C NMR** (63 MHz, $CDCl_3$): δ 144. 5 (Car), 140.3 (Car), 128.6 (Car), 127.4 (Car), 126.1 (Car), 124.7 (CF_3), 124.2 (Car), 120.1 (CF_3), 86.4 (C, $C(CF_3)_2OH$), 76.0 (C, CHO), 74.2 (C≡C), 70.3 (C≡C), 34.3 (CH_2), 31.6 (CH_2), 22.1 (CH_2), 20.6 (CH_2), 10.0 (CH_3). **IR** (film, cm^{-1}): 3285, 2967, 2933, 2879, 1206, 1150. **HRMS** ([ESI-TOF]$^+$, m/z) $[M+H]^+$ calcd for $C_{17}H_{18}O_2F_6Na$, 391.1103; found 391.1116.

18c [0.143g, 90%, R_f = 0.40 (50% EtOAc/hexanes), colorless oil]. **^{1}H NMR** (250 MHz, $CDCl_3$): δ 7.20 (m, 4H), 4.85 (q, *J* = 6.4, 1H, CHOH), 3.71 (br s, 1H, OH), 2.80 (m, 4H), 2.51 (m, 2H), 2.01 (br s, 1H, OH), 1.47 (d, *J* = 6.4, 3H).**^{13}C NMR** (63 MHz, $CDCl_3$): δ 145. 7 (Car), 140.3 (Car), 129.2 (Car) 128.6 (Car), 127.3 (Car), 125.5 (Car), 124.7 (CF_3), 123.6 (Car), 120.1 (CF_3), 86.3 (C, $C(CF_3)_2OH$), 82.6 (C≡C), 77.1 (C≡C), 70.3 (C, CHOH), 34.2 (CH_2), 24.7 (CH_3), 22.0 (CH_2), 20.5 (CH_2). **IR** (film, cm^{-1}): 3493, 2961, 2940, 2163, 1203, 1207. **HRMS** ([ESI-TOF]$^+$, m/z) $[M+H]^+$ calcd for $C_{16}H_{16}O_2F_6Na$, 377.0952; found 377.0947.

8b [0.093 g, 94 %, R_f = 0.55 (30% EtOAc/hexanes), colorless oil]. **^{1}H NMR** (250 MHz, $CDCl_3$): δ 7.82 (m, 2H), 7.66 (m, 2H), 3.92(br s, 1H, OH), 3.00 (qd, J_1 = 7.2, J_2 = 1.3, 2H, CH_2-Me), 2.87 (m, 4H, 2XCH_2), 2.54 (t, *J* = 6.2, 2H), 1.22 (td, J_1 = 7.3, J_2 = 1.3, 3H). **^{13}C NMR** (63 MHz, $CDCl_3$): δ 201.4 (C=O), 140.6 (Car), 137.0 (Car), 133.0 (Car), 128.6 (Car), 127.9 (Car), 126.2 (Car), 124.7 (CF_3), 120.1 (CF_3), 86.0 (C, $C(CF_3)_2OH$), 74.4 (C≡C), 70.5(C≡C), 34.1 (CH_2), 31.7 (CH_2), 22.1 (CH_2), 20.4 (CH_2), 8.1 (CH_3). **IR** (film, cm^{-1}): 3355, 2981, 2939, 2875, 2356, 1676, 1204. **HRMS** ([ESI-TOF]$^+$, m/z) $[M+H]^+$ calcd for $C_{17}H_{17}O_2F_6$, 367.1127; found 367.1129.

8c [0.34 g, 95 %, R_f = 0.55 (30% EtOAc/hexanes), colorless oil]. **^{1}H NMR** (250 MHz, $CDCl_3$): δ 7.79 (m, 2H), 7.40 (m, 2H), 4.11(br s, 1H, OH), 2.86 (m, 4H, 2XCH_2), 2.59 (s, 3H, Me), 2.53 (m, 2H).**^{13}C NMR** (63 MHz, $CDCl_3$): δ 198.8 (C=O), 140.6 (Car), 137.1 (Car), 133.1 (Car), 128.6 (Car), 128.0 (Car), 126.7 (Car), 124.7 (CF_3), 120.1 (CF_3), 85.6 (C, $C(CF_3)_2OH$), 70.6 (C≡C), 64.4(C≡C), 34.1 (CH_2), 26.3 (CH_3), 22.1 (CH_2), 20.4 (CH_2).**IR** (film, cm^{-1}): 2927, 2898, 2875, 2022, 1740, 1208. **HRMS** ([ESI-TOF]$^+$, m/z) $[M+H]^+$ calcd for $C_{16}H_{14}O_2F_6Na$, 375.0796; found 375.0790.

19b. [0.118g, 90%, R_f = 0.55 (20% EtAc/hexanes), colorless oil]. **^{1}H NMR** (250 MHz, $CDCl_3$): δ 7.77 (m, 2H), 7.33 (m, 2H), 2.97 (q, *J* = 7.2, 2H), 2.81 (m, 4H, 2XCH_2), 2.46 (t, *J* = 7.5, 2H), 1.19 (t, *J* = 7.2, 3H, Me), 0.91 (m, 9H, $(CH_3CH_2)_3Si$), 0.62 (m, 6H, $(CH_2)_3Si$). **^{13}C NMR** (63 MHz, $CDCl_3$): δ 200.1 (C=O), 140.8 (Car), 137.1 (Car), 132.8 (Car), 128.4 (Car), 127.7 (Car), 125.9 (Car), 124.8 (CF_3), 120.2 (CF_3), 83.6 (C, COTES), 77.4 (C≡C), 71.8 (C≡C), 34.5 (CH_2), 31.6 (CH_2), 22.9 (CH_3), 20.6 (CH_2), 8.1 (CH_3), 6.2 (CH_3), 5.7 (CH_2). **IR** (film, cm^{-1}): 3447, 3238, 2948, 2325, 1635, 1209. **HRMS** ([ESI-TOF]$^+$, m/z) $[M+H]^+$ calcd for $C_{23}H_{31}O_2F_6Si$, 481.1992; found 481.1978.

19c [0.120g, 91%, R_f = 0.55 (20% EtAc/hexanes), colorless oil]. **^{1}H NMR** (250 MHz, $CDCl_3$): δ 7.76 (m, 2H), 7.36 (m, 2H), 2.80 (m, 4H, 2XCH_2), 2.56 (s, 3H, Me), 2.53 (m, 2H), 0.93 (m, 9H, 3xCH_3CH_2Si), 0.60 (m, 6H, 3xCH_2Si). **^{13}C NMR** (63 MHz, $CDCl_3$): δ 198.0 (C=O), 140.8 (Car), 137.1 (Car), 133.0 (Car), 128.4 (Car), 127.9 (Car), 126.3 (Car), 124.7 (CF_3), 120.0 (CF_3), 83.4 (C≡C), 77.3 (C, COTES), 71.8 (C≡C), 34.4 (CH_2), 26.3 (CH_3), 22.9 (CH_2), 20.5 (CH_2), 6.3 (CH_3), 5.6 (CH_2). **IR** (film, cm^{-1}): 2930, 2878, 2856, 2122, 1742, 1210. **HRMS** ([ESI-TOF]$^+$, m/z) $[M+H]^+$ calcd for $C_{22}H_{28}F_6O_2SiNa$, 489.1660; found 489.1656.

3b [26 mg, 32%, R_f = 0.38 (50% EtOAc/hexanes), white foam purified by HPLC (Phenomenex SiO_2, Luna Silica(2) 5μ, 250 x 10 mm, 10% *i*-PrOH/hexanes). $[\alpha]_D^{25}$ = +16.8° (c = 5 in EtOH). UV (96% EtOH): λmax: 298 nm (ε = 13.037). **^{1}H NMR** (250 MHz, $CDCl_3$): δ 7.23 (m, 3H), 7.05 (m, 1H), 6.74 (d, *J* = 11.4, 1H, H-7), 6.43 (d, *J* = 11.4, 1H, H-6), 5.35 (s, 1H, H-19), 5.04 (s, 1H, H-19), 4.46 (t, *J* = 5.6, 1H, H-1), 4.25 (m, 1H, H-3), 2.81 (m, 4H), 2.66 (dd, J_1 = 13.2, J_2= 3.5, 1H), 2.51 (m, 2H), 2.37 (dd,

J_1 = 13.2, J_2= 7.1,1H), 2.16 (s, Me), 1.98 (t, J = 5.6, 2H),1.63 (br s, 3H-3OH). **^{13}C NMR** (63 MHz,$CDCl_3$): δ 147.0 (=C), 143.6 (=C), 140.0 (=C), 136.6 (=C), 135.8 (CH), 128.2 (CH), 126.8 (CH), 126.4 (CH), 125.7 (CH), 125.6 (CH), 124.7 (C-F) 123.8 (CH), 123.5 (CH) 120.15 (C-F), 113.0 (=C,C-19), 86.0 (C, COH), 76.3 (C≡), 70.9 (CH, C-1), 70.2 (C≡), 66.6 (CH, C-3), 45.1 (CH_2), 42.5 (CH_2), 34.4 (CH_2), 22.1 (CH_2), 20.5 (CH_2), 15.8 (CH_3). **IR** (film, cm^{-1}): 3367, 2965, 2930, 2855, 1376, 1212. **HRMS** ([ESI-TOF]$^+$, m/z) $[M+H]^+$ calcd for $C_{25}H_{26}O_3F_6Na$, 511.1684; found 511.1680.

3c [32 mg, 27%, R_f = 0.38 (50% EtOAc/hexanes), foam purified by HPLC (Phenomenex SiO_2, Luna Silica(2) 5μ, 250 x 10 mm, 10% *i*-PrOH/hexanes). $[\alpha]_D^{25}$ = +12.8° (c = 5 in EtOH). UV (96% EtOH): λmax: 298 nm (ε= 12600). **^{1}H NMR** (250 MHz, $CDCl_3$): δ 7.21 (m, 3H), 7.06 (m, 1H), 6.61 (d, J = 11.4, 1H, H-7), 6.42 (d, J = 11.4, 1H, H-6), 5.33 (s, 1H, H-19), 5.03 (s, 1H, H-19), 4.45 (t, J = 5.6, 1H, H-1), 4.23 (m, 1H, H-3), 3.69 (br s, 1H, H-OH), 2.80 (m, 4H), 2.64 (dd, J_1 = 14.9, J_2= 7.5, 1H), 2.51 (m, 2H), 2.36 (dd, J_1 = 13.2, J_2= 7.1,1H), 1.97 (t, J = 5.6, 2H), 1.74 (br s, 3H-3OH), 1.03 (t, J = 7.5, 3H, Me). **^{13}C NMR** (63 MHz,$CDCl_3$): δ 147.0 (=C), 142.7 (=C), 142.6 (=C), 139.9 (=C), 136.5 (=C), 128.3 (CH), 126.6 (CH), 126.0 (CH), 125.4 (C-F), 124.3 (CH), 122.9 (C-F) 112.9 (C-19), 86.6 (C, COH), 76.8 (C≡), 71.0 (CH, C-1), 69.9 (C≡), 66.6 (CH, C-3), 45.3 (CH_2), 42.6 (CH_2), 34.4 (CH_2), 22.9 (CH_2), 22.1 (CH_2), 20.5 (CH_2), 13.7 (CH_3). **IR** (film, cm^{-1}): 3498, 3008, 2932, 2883, 1210. **HRMS** ([ESI-TOF]$^+$, m/z) $[M+H]^+$ calcd for $C_{26}H_{28}O_3F_6Na$, 525.18349; found 525.18336.

Cell Culture and treatments. The human breast adenocarcinoma MDA-MB-231 and MCF-7 cell lines, and the normal human keratinocytes HaCaT cells were obtained from ATCC-LGC (Barcelona, Spain). Cells were grown as previously described.[25] Cells were plated and cultured in a medium supplemented with charcoal-treated FCS to remove liposoluble hormones, and 24 h later treated either with 1,25D_3 (**1)** or the **2**, **3a**, **3b** and **3c** compounds. All the compounds were dissolved in ethanol.

Cell Proliferation and three-dimensional (3D) cultures.

MDA-MB-231 and HaCat cells (2 x105 cells/well) were treated with **1** and the **2**, **3a**, **3b**, and **3c** analogs at 10^{-7} M for 48 h, and MTT (Merck, Darmstadt, Germany) was added. The medium was removed and cells were solubilized with DMSO and absorbance was measured at 570 nm in a Mithras LB 940 from Berthold Technologies (Bad Wildbad, Germany). For 3D cultures, a single-cell suspension containing 5x10^3 of MDA-MB-231

cells/100 µL was placed on a 96-well plate cell-repellent surface (Greiner Bio-One, Germany) for 4 days and then treated with ethanol (control), cisplatin (25 µM, Pfizer S.L., Madrid, Spain), **1**, **2**, **3a**, **3b** and **3c** (all at 10^{-7} M), and both cisplatin + **1** or the **2**, **3a**, **3b** and **3c** analogs for 6 days. Phase-contrast microphotographs were taken with an Olympus DP72 camera. Cell growth was quantitated by measuring the sphere diameter. At least eight spheres were scored for each condition.

Real-Time PCR and Western blot. MCF-7 cells were treated with **1** and the **2**, **3a**, **3b** and **3c** analogs at 10^{-7} M. Isolation of total RNA was performed using TRIzol reagent (Invitrogen, Barcelona, Spain), and cDNA synthesis was carried out using 1 µg of total RNA. cDNA was used for *CYP24A1* (24-hydroxylase) quantification by real-time PCR (Eppendorf Master cycler ep realplex, Hamburg, Germany) using Luminaris Color HiGreen qPCR Master Mix (Thermo Fisher Scientific, Barcelona, Spain) as previously described.[43] Protein expression of E-cadherin (BD Biosciences, Franklin Lakes, USA) and GAPDH (Santa Cruz Biotechnology, XX, USA, as loading control) in MCF-7 cells treated with ethanol, **1** and the **2**, **3a**, **3b** and **3c** analogs (10^{-7} M for 48 h) was performed by Western blot as previously described[44] and quantified using ImageJ software (National Institutes of Health, Bethesda, USA).

Human VDR Binding Assay. VDR binding was evaluated as previously described.[25] The activity of each compound is shown as a percentage, in which the activity of the 1 was normalized to 100%.

Serum calcium evaluation. All animal studies were approved by the University of Santiago de Compostela Ethics Committee for Animal Experiments. Compounds **1**, **2**, **3a**, **3b**, and **3c** (0.3 µg/kg weight) were injected intraperitoneally (i.p) in groups of 5 male Swiss cd-1 mice. The injections were performed every other day for 21 days using sesame oil as a vehicle. At the end of the test, the weight of the animals was evaluated, and serum calcium was determined using the QuantiChom calcium assay kit (BioAssay Systems, Hayward, USA).

Biochemistry, Crystallization, and Structure Determination. The His-tagged zVDR LBD (156-453) was expressed and purified as previously described.[25] The concentrated purified proteins were incubated with a 2-fold excess of ligand and a 3-fold excess of the coactivator NCOA2 NR2 (KHKILHRLLQDSS) peptide. Crystals of VDR-**2** were grown at 293K in $LiSO_4$ 1.6M, Hepes 0.1M pH 7.5 and were mounted in a fiber loop and flash-cooled under a nitrogen flux after cryoprotection with $LiSO_4$ 2.2M, BisTris 0.1M pH 7.

Crystals of VDR-**3a** and VDR-**3b** were obtained at 293K in NaAcetate 2.5M, BisTris 0.1M pH 7 and were mounted in a fiber loop and cryoprotected with NaAcetate 3M, BisTris 0.1M pH 7. Crystals of VDR-**3c** were grown at 293K in NH_4SO_4 1.5M, BisTris 0.1M pH 7 and were mounted in a fiber loop and flash-cooled under a nitrogen flux after cryoprotection with $LiSO_4$ 2.2M, BisTris 0.1M pH 7. Data collections from a single frozen crystal were performed at 100 K on the ID30b at ESRF (France). The crystallographic raw data were processed with XDS[45] and scaled with AIMLESS[46] programs. The crystals belong to the space group $P6_522$, with one LBD complex per asymmetric unit. The structures were solved and refined using Phenix[47] and iterative model building using COOT.[48] Crystallographic refinement statistics are presented in Supplementary Table S1.

Supporting Information.

Additional supplemental figures and tables, synthetic procedures, and purity HPLC traces and characterization data for compounds can be found in SI appendix.

Molecular formula strings (CSV) with biochemical source data (CSV).

3D model files of the docking.

3D models after 20ns MD.

Accession Codes. Atomic coordinates for the X-ray structure of zVDR LBD-**2** (PDB 8PWF), zVDR LBD-**3a** (PDB 8PWE), zVDR LBD-**3b** (PDB 8PWM) and zVDR LBD-**3c** (PDB 8PWD) are available from the RCSB Protein Data Bank.

Notes

The authors declare no competing financial interest.

ACKNOWLEDGMENTS

We thank the Xunta de Galicia (GRC/ED431B/2021/004 to AM and RP-F), and MICIN/AEI/PGC2018-100776-B-I00 and MICIN/AEI/PID2021-127394OB-100 to RP-F. This work was supported by INSERM, CNRS, Unistra and IGBMC, the French state funds from Agence Nationale de la Recherche (ANR-21-CE17-0009-01 to N.R.), and institutional funds from Instruct-ERIC for support and the use of resources of the French Infrastructure for Integrated Structural Biology (ANR-10-LABX-0030-INRT and ANR-10-IDEX-0002-02). We thank the German Academic Exchange Service (DAAD) for

granting a fellowship. We thank CESGA for the computing time. The authors would like to thank the staff of ID30b at ESRF for assistance in using the beamlines and Alastair McEwen (IGBMC) for help in X-ray data collections.

ABBREVIATIONS USED

$1,25D_3$, 1α,25-dihydroxyvitaminD_3; LBD, ligand binding domain; MD, molecular dynamics; VDR, vitamin D receptor

REFERENCES

1. Fleet, J. C. The role of vitamin D in the endocrinology controlling calcium homeostasis. *Mol. Cell Endocrinol.* **2017**, *453*, 36-45.

2. Goltzman, D. Functions of vitamin D in bone. *Histochem. Cell Biol*. **2018**, *149*, 305-312.

3. Christakos, S.; Dhawan, P.; Verstuyf, A.; Verlinden, L.; Carmeliet, G. Vitamin D: Metabolism, molecular mechanism of action, and pleiotropic effects. *Physiol. Rev*. **2016**, *96*, 365-408.

4. Chen, J.; Tang, Z.; Slominski, A. T.; Li, W.; Zijewski, M. A.; Liu, Y.; Chen. J. Vitamin D and its analogs as anticancer and anti-inflammatory agents. *Eur. J. Med. Chem*. **2020**, *207*, 112738.

5. Tiosano D, Abrams SA, Weisman Y. Lessons learned from hereditary 1,25-dihydroxyvitamin D-resistant rickets patients on vitamin D functions. *J. Nutr*. **2021,** *151*, 473-481.

6. Tagliabue, E.; Raimondi, S.; Gandini, S. Meta-analysis of vitamin D-binding protein and cancer risk. *Cancer Epidemiol. Biomarkers Prev*. **2015**, *24*, 1758-1765.

7. Feldman, D.; Krishnan, A.V.; Swami, S.; Giovannucci, E.; Feldman, B. J. The role of vitamin D in reducing cancer risk and progression. *Nat. Rev. Cancer* **2014**, *4*, 342–357.

8. Carlberg, C.; Muñoz, A. An update on vitamin D signaling and cancer. *Semin. Cancer Biol.* **2022**, *79*, 217-230.

9. Jones, G.; Kaufmann, M. Update on pharmacologically-relevant vitamin D analogues. *Br. J. Pharmacol.* **2019**, *85*, 1095-1102.

10. Maestro, M. A.; Molnár, F.; Carlberg, C. Vitamin D and its synthetic analogs. *J. Med. Chem.* **2019**, *62*, 6854-6875.

11. Belorusova, A. Y.; Rochel, N. Structural studies of vitamin D nuclear receptor ligand-binding properties. *Vitam. Horm*. **2016**, *100*, 83-116.

12. Bouillon, R.; Okamura, W. H.; Norman, A. W. Structure-function relationships in the vitamin D endocrine system. *Endocr. Rev.* **1995**, *16*, 200-256.

13. Glebocka, A.; Chiellini, G. A-ring analogs of 1,25-dihydroxyvitamin D_3. *Arch. Biochem. Biophys.* **2012**, *523*, 48-57.

14. Zhu, G. D.; Okamura, W. H. Synthesis of Vitamin D (Calciferol). *Chem. Rev*. **1995**, *95*, 1877-1952.

15. Krause, S.; Schmalz, H. -G. *Organic synthesis highlights* (Ed: H.- G. Schmalz), Wiley and VCH: Weinheim, Germany, **2000**, pp 212-217.

16. Chapelon, A. S.; Moraleda, D.; Rodríguez, R.; Ollivier, C.; Santelli. M. Enantioselective synthesis of steroids. *Tetrahedron* **2007**, 11511-11616.

17. López-Pérez, B.; Maestro, M.; Mouriño, A. Total synthesis of 1α,25-dihydroxyvitamin D_3 (calcitriol) through a Si-assisted allylic substitution. *Chem. Commun.* **2017**, *53*, 8244-8147.

18. Fernández, S.; Ferrero, M.; Strategies for the synthesis of 19-nor-vitamin D analogs. *Pharmaceuticals* **2020**, *13,* 159.

19. Eelen, G.; Verlinden, L.; Bouillon, R.; DeClercq, P.; Muñoz, A.; Verstuyf, A. CD-ring modified vitamin D_3 analogs and their superagonistic action. *J. Steroid Biochem. Mol. Biol*. **2010**, *121*, 417-419 and ref. therein.

20. Bolla, N. R.; Marcinkowska, E.; Brown, G.; Kutner, A. Retiferols - synthesis and biological activity of a conceptually novel class of vitamin D analogs. *Expert Opin. Ther. Pat.* **2014**, *24*, 1-14 and ref. therein.

21. Carballa, D. M.; Seoane, S.; Zacconi, F.; Pérez, X.; Rumbo, Álvarez-Díaz, S.; Larriba, M. J.; Pérez-Fernández, R.; Muñoz, A.; Maestro, M.; Mouriño, A.; Torneiro, M. Synthesis and biological evaluation of 1α,25-dihydroxyvitamin D_3 analogues with long side chain at C12 and short C17 side chains. *J. Med. Chem.* **2012**, *55*, 8642–8656 and ref. therein.

22. Kawagoe, S.; Mototani, S.; Kittaka, A. The synthesis and biological evaluation of D-ring-modified vitamin D analogues. *Biomolecules* **2021**, *11*, 1639 and ref. therein.

23. Laplace, D. R.; Overschelde, M. V.; De Clercq, P.; Verstuyf, A.; Winne, J. M. Synthesis of 2-ethyl-19-nor-analogs of 1α,25-dihydroxyvitamin D_3. *Eur. J. Org. Chem*. **2013**, 728-735.

24. Gogoi, P.; Seoane, S.; Sigüeiro, R.; Guiberteau, T.; Maestro, M. A.; Pérez-Fernández, R.; Rochel, N.; Mouriño, A. Aromatic-based design of highly active and noncalcemic vitamin D receptor agonists. *J. Med. Chem*. **2018**. *61*, 4928-4937.

25. Seoane, S.; Gogoi, P.; Zárate-Ruíz, A.; Peluso-Iltis, C.; Peters, S.; Guiberteau, T.; Maestro, M. A.; Pérez-Fernández, R.; Rochel, N.; Mouriño, A. Design, synthesis, biological activity, and structural analysis of novel des-C-ring and aromatic-D-ring analogues of 1α,25-dihydroxyvitamin D_3 *J. Med. Chem*. **2022**, 65, 13112–13124.

26. Jones, G. Analog metabolism. In Vitamin D; Feldman, D., Glorieux, F. H., Pike, J. W., Eds.; Academic Press: San Diego, CA, 1997; Vol. 61, pp 973−994.

27. Y. Wu, P. De Clercq, M. Vandewalle, R. Bouillon, A. Verstuyf. Vitamin D_3: Synthesis of seco-C-9,11-bisnor-17-methyl-1α,25-dihydroxyvitamin D_3 Analogues. Bioorg. Med. Chem. Lett. **2002**, *12,* 1633-1636.

28. Rhieu, S. Y.; Annalora, A. J.; Gathungu, R. M.; Vouros, P.; Milan R. Uskokovic, M. R.; Schuster, I.; Tayhas G.; Palmore, R.; Satyanarayana Reddy, G. S. A new insight into the role of rat cytochrome P450 24A1 in metabolism of selective analogs of 1α,25-dihydroxyvitamin D_3. *Arch. Biochem. Biophys*. **2011**, *509*, 33–43.

29. Eelen, G.; Valle, N.; Sato, Y.; Rochel, N.; Verlinden, L.; De Clercq, P. D. Moras, D. Superagonistic fluorinated vitamin D_3 analogs stabilize helix 12 of the vitamin D receptor. *Chem. Biol.* **2008**, *15*, 1029-1034.

30. Karagoe, F.; Mototani, S.; A. Kittaka, A. Design and synthesis of fluoro analogues of vitamin D. *In. Mol. Sci.* **2021**, *22,* 8191

31. Eberhardt, J.; Santos-Martins, D.; Tillack, A. F.; Forli, S. AutoDock Vina 1.2.0: New docking methods, expanded force field, and python bindings. *J. Chem. Inf. Model*. **2021**, *61*, 3891–3898.

32. Rochel, N.; Wurtz, J. M.; Mitschler, A.; Klaholz, B.; Moras, D. The crystal structure of the nuclear receptor for vitamin D bound to its natural ligand. *Mol. Cell* **2000**, *5*, 173–179.

33. Krieger, E.; Vriend, G. New ways to boost molecular dynamics simulations. *J. Comput. Chem.* **2015**, *36,* 996-1007.

34. Krieger, E.; Vriend, G. J. YASARA View-molecular graphics for all devices-from smartphones to workstations. *Bioinformatics* **2014**, *30*, 2981– 2982.

35. For a review on the Lythgoe's Wittig-Horner approach to vitamin D, see: Lythgoe, B. Synthetic approaches to vitamin D and its relatives. *Chem. Soc. Rev.* **1980**, *9,* 449-475.

36. Corey, E. J.; Fuchs, P. L. A synthetic method for formyl-ethynyl conversion. *Tetrahedron Lett.* **1972,** *13*, 3769-3772.

37. Dess, D. B.; Martin, J. C. Readily accessible 12-I-5 oxidant for the conversion of primary and secondary alcohols to aldehydes and ketones. *J. Org. Chem.* **1983**, *48*, 4155-4156.

38. F. Ciesielski, N. Rochel, D. Moras. Adaptability of the vitamin D nuclear receptor to the synthetic ligand Gemini: remodelling the LBP with one side chain rotation. *J. Steroid Biochem. Mol. Biol.* **2007**, *103*, 235-242.

39. Sigüeiro, R.; Bianchetti, L.; Peluso-Iltis, C.; Chalhoub, S.; Dejaegere, A.; Osz, J.; Rochel, N. Advances in vitamin D receptor function and evolution based on the 3D structure of the lamprey ligand-binding domain. *J Med Chem*. **2022**, 65, 5821-5829.

40. Belorusova, A.Y.; Chalhoub, S.; Rovito, D.; Rochel, N. Structural analysis of VDR complex with ZK168281 antagonist. *J. Med. Chem*. **2020**, *63*, 9457-9463.

41. Rovito, D.; Belorusova, A. Y.; Chalhoub, S.; Rerra, A.I.; Guiot, E.; Molin, A.; Linglart, A.; Rochel, N.; Laverny, G.; Metzger, D. Cytosolic sequestration of the vitamin D receptor as a therapeutic option for vitamin D-induced hypercalcemia. *Nat. Commun.* **2020**, *11*, 6249.

42. Biediger, R. J.; Chen, Qi; Decker, E. R.; Holland, G. W.; Kassir, J. M.; Li, W.; Market, R. V.; Scott, I. L.; Wu, C.; Li, J. Preparation of carboxylic acid derivatives that inhibit the binding of integrins to their receptors. United States, US20040063955 A1 2004-04-01.

43. Martínez-Ordoñez, A.; Seoane, S.; Avila, L.; Eiro, N.; Macía, M.; Arias, E.; Pereira, F.; García-Caballero, T.; Gómez-Lado, N.; Aguiar, P.; Vizoso, F.; Pérez-Fernández, R. POU1F1 transcription factor induces metabolic reprogramming and breast cancer progression via LDHA regulation. *Oncogene* **2021**, *40*, 2725-2740.

44. Seoane, S.; Martinez-Ordoñez, A.; Eiro, N.; Cabezas-Sainz, P.; Garcia-Caballero, L.; Gonzalez, L. O.; Macia, M.; Sanchez, L.; Vizoso, F.; Perez-Fernandez, R. POU1F1 transcription factor promotes breast cancer metastasis via recruitment and polarization of macrophages. *J. Pathol*. **2019**, *249*, 381-394.

45. Kabsch, W. Software XDS for image rotation, recognition and crystal symmetry assignment. *Acta Crystallogr., Sect. D: Biol. Crystallogr.* **2010**, *66*, 125−132.

46. Evans, P. Scaling and assessment of data quality. *Acta Crystallogr. Sect. D: Biol. Crystallogr*. **2006**, *62*, 72−82.

47. Afonine, P. V.; Grosse-Kunstleve, R. W.; Adams, P. D. *CCP4 Newsletter* **2005**, *42*. contribution 8.

48. Emsley, P.; Cowtan, K. Coot: model-building tools for molecular graphics. *Acta Crystallogr. Sect. D: Biol. Crystallogr.* **2004**, *60*, 2126−2132.